APPLICATIONS OF TEXTURE ANALYSIS FOR ROCK TYPES DISCRIMINATION PHASE II

Final Technical Report

SHIN-YI HSU, Ph.D.
Susquehanna Resources and Environment, Inc.
305 Main Street
Johnson City, New York 13790

Sponsored by:

Advanced Research Projects Agency (DOD)
ARPA Order No. 4288

Monitored by AFOSR Under Conrtact No. F 49620-83-C-0029
Bolling Air Force Base, D.C. 20332

SUSQUEHANNA RESOURCES AND ENVIRONMENT, INC.
305 Main Street
Johnson City, New York 13790
Telephone: (607) 729-6671

PREFACE

This research was sponsored by the Advanced Research Projects Agency under the monitorship of Mr. William Best of Air Force Office of Scientific Research. Dr. Shin-yi Hsu is the principal investigator. Research scientists of the project include Dr. Timothy Masters and Ms. Jane Huang of Susquehanna Resources and Environment, Inc.

Mr. Jack Rachlin and his associates at U.S. Geological Survey served as the reviewer of the effort. Lt. Colonel James Smith of AFOSR served as technical adviser; his assistance to the project is highly appreciated.

Phase I technical report has been read by Dr. Mark Settle of the NASA Headquarters, and Dr. Jack Paris of Jet Propulsion Laboratory, California Institute of Technology. This technical report has taken into consideration their comments regarding particularly the use of the ordinary geologic maps as the ground truth information of the LANDSAT data, and background information on textural algorithms for lithologic analysis.

Unclassifi

SECURITY CLASSIFICATION OF THIS PAGE (When Data Entered)

REPORT DOCUMENTATION PAGE	READ INSTRUCTIONS BEFORE COMPLETING FORM
1. REPORT NUMBER AFOSR-TR- 84-0477 / 2. GOVT ACCESSION NO. A142268	3. RECIPIENT'S CATALOG NUMBER
4. TITLE (and Subtitle) Applications of Texture Analysis for Rock Types Discrimination: Phase II	5. TYPE OF REPORT & PERIOD COVERED Final Report Nov. 1982 - Nov. 1983
	6. PERFORMING ORG. REPORT NUMBER
7. AUTHOR(s) Shin-yi Hsu, Ph.D.	8. CONTRACT OR GRANT NUMBER(s) Contract F49620-83-C-0029
9. PERFORMING ORGANIZATION NAME AND ADDRESS Susquehanna Resources and Environment, Inc. 305 Main Street Johnson City, New York 13790	10. PROGRAM ELEMENT, PROJECT, TASK AREA & WORK UNIT NUMBERS 61102F ARPA No. 4288
11. CONTROLLING OFFICE NAME AND ADDRESS Air Force Office of Scientific Research Bolling Air Force Base Washington, D.C. 20332	12. REPORT DATE December, 1983
	13. NUMBER OF PAGES
14. MONITORING AGENCY NAME & ADDRESS(if different from Controlling Office)	15. SECURITY CLASS. (of this report) Unclassified
	15a. DECLASSIFICATION/DOWNGRADING SCHEDULE

16. DISTRIBUTION STATEMENT (of this Report)

Approved for public release; distribution unlimited

17. DISTRIBUTION STATEMENT (of the abstract entered in Block 20, if different from Report)

18. SUPPLEMENTARY NOTES

19. KEY WORDS (Continue on reverse side if necessary and identify by block number)

Rock types discrimination	Region growing	LANDSAT data
Granite	Supervised classification	Band ratioing
Texture analysis	Clustering analysis	Nuclear monitoring
Smart algorithms	Quarternary geologic maps	

20. ABSTRACT (Continue on reverse side if necessary and identify by block number)

Aimed at developing image processing methods for rock types analysis with LANDSAT data, numerous experiments were conducted using supervised and unsupervised classification techniques under the general concept of texture analysis with LANDSAT digital data covering two geological quads of Nevada.

The results indicate that the supervised classification method is

DD FORM 1 JAN 73 1473 EDITION OF 1 NOV 65 IS OBSOLETE

UNCLASSIFIED

SECURITY CLASSIFICATION OF THIS PAGE (When Data Entered)

very effective in the extraction of granite regions when (1) data were in ratio format, (2) feature variables included both tone and texture information, and (3) the classifier is capable of handling non-normally distributed data. Classification errors occurred when there exists pixels of non-granite category whose spectral and textural properties are statistically similar to that of granite pixels. Two cases of errors can be noted: Type 1 pixels located at the periphery of the granite regions, and Type 2 pixels located far away from the core of the granite areas.

To reduce the error rate, an unsupervised classification method based on the concept of region growing and texture clustering analysis was employed to segment the scene in multiple stages and thus depict edge patterns by the scene content and a gradual mathematical generalization process. Identification of the grantie regions becomes a labeling process using the training sets information. Since the Regions algorithm is based on an additional constraint on spatial contiguity, the above-mentioned two types of errors can be effectively reduced bacause sharp edges exist between the granite and non-granite pixels in the study area.

The final decision regarding the delineation of the granite regions is based on the intersection of two classification maps using a simple map overlay analysis. The result yields a correct classification rate of about 95 percent based on a visual comparision between the composite classification map and the ground truth information given in the U.S.G.S. geological map of the study area.

To improve the developed techniques for lithological analysis, it is recommended that additional experiments be conducted using other regions in the United States centering around the following tasks:

(1) developing algorithms for merging supervised and unsupervised classification methods;
(2) finetuning the Region algorithm by adding subroutings to output digital information of each segmented region;
(3) developing a color prediction model for rock types identification using the texture and tone information in the color domain with a color monitor; and
(4) developing change detection methods for monitoring purposes based on the extension of the above three methods.

The above discussions apply to our Phase I effort. The Phase II investigation is designed to test the generalizability of the methodologies developed from the Phase I experiments. In general, it has been proven that they are indeed generalizable with the following qualifications:

(1) The ratio bands are not an absolute requirement;
(2) Our unsupervised classification method has been improved substantially to the point that it can be used as a smart processor for extracting alluvium automatically; and
(3) Quarternary geologic maps are more appropriate than the ordinary geologic maps for serving as the ground truth information of the LANDSAT data.

The directions of future research should be centered around the development of smart algorithms based on our thorough understanding of the physical processes by which the terrain units were derived.

TABLE OF CONTENT

Executive Summary

It has been determined in the literature on seismology and geophysics that the recorded seismic wave energy from nuclear explosions is highly dependent upon the actual yield of the explosion and its interaction with the environments in which the detonation occurs. These environmental factors can be characterized by the depth of explosion below the surface, the degree of coupling between the charge and the adjacent medium, and the lithological nature of the test sites. Therefore, the analysis of rock type at the test sites is the first step in nuclear monitoring.

The LANDSAT data have been determined effective for terrain analysis. The choice of the LANDSAT imagery for rock types analysis at the nuclear test sites is also based upon the fact that it can provide world-wide coverage with repetitive observatoins for monitoring purposes. And in certain cases, only a combination of seismic and LANDSAT imagery can yield significant information on geology and tectronics that either alone would not provide (Pavlin and Langston, 1983). The goal of this study is to test the generalizability of utilizing LANDSAT's digital, multispectral information for rock types discrimination at the nuclear test sites, based on the texture-tone analysis algorithms of the image processing systems at Susquehanna Resources and Environment, Inc. in two complementary approaches: supervised classifaction and unsupervised training methodology.

The experiments were based on two subframes of LANDSAT MSS data covering two geological quadrangles: Site 1 located in the Duffer Peak Quad, Nevada, and Site 2 uses the NE quarter of the Willow Spring and Rosamond Quads of California. In addition to determining the general capability and generalizability of the texture analysis algorithm from Site 1 to Site 2, this study also tests the appopriateness of using a general geologic map as the ground

truth for judging the feature extraction capability of the LANDSAT data based particularly on Site 2 where a quarternary geologic map happens to be available to the researchers.

The task was accomplished by using two separate but complementary image processing techniques. The first technique, a supervised classification, was designed to extract granite regions using four ratio bands (4/7, 4/6, 5/7, and 6/7) for the Duffer Peak Site, and four original bands for the Rosamond Site based upon four manually selected, but automatically pre-processed training sets. The non-granite regions were extracted as well using the reject category of the classification model. The second method, an unsupervised classification procedure based on the concepts of the stable structure of scenes (Hsu, 1983), was designed to detect the contact zones between granite regions and the algorithm using one ratio band (4/7 is most effective) of the Duffer Peak Site, where the supervised method failed.

For Site 1 (Duffer Peak, Nevada), the final granite regions were defined by the intersection of two granite images produced by two different image analysis techniques. The result indicates that a very high level of correct classification rate--95 percent or better--has been achieved, based on an overlay analysis using the classification result against the geologic map produced by the U.S. Geological Survey.

For Site 2 (Rosamond, California), the granite regions are successfully extracted using the raw LANDSAT MSS information based upon the same variables and classifier employed in Site 1; and thus proving the generalizability of the developed methodologies for rock types discrimination.

On the appropriateness of using the general geologic map as the ground truth for judging the performance of the LANDSAT system, we have determined that a Quartenary geologic map where information on the properties of surfi-

cial (soil) material is availabe is much more appropriate than the general geologic map where the distributions of rocks is mapped according to mainly the interpretation of the distribution of the bedrocks by the particular field geologists. Moreover the LANDSAT system is really not designed for detecting sub-surface material although the sub-surface information can sometimes be inferred from the surficial expression of the terrain characteristics as captured in the LANDSAT imagery through image processing and analysis.

Though the defined task of extracting granite regions has been successfully accomplished, it is necessary to test the developed image processing and analysis techniques using additional test sites. The reasons are (1) fine tuning of the methods are usually required to handle diverse patterns of lithological associations, and (2) the LANDSAT imagery can be exploited further for detecting environmental and man-made changes before and after nuclear explosions, but it has not been fully investigated by the researschers at Susquehanna Resources & Environment, Inc.

Applications of Texture Analysis for Rock Types Discrimination: Phase II

Section A: Introduction

Ever since the Soviet Union's detonation of its first nuclear device prototypes, both the realities of an arms race and the requirement to maintain scientific/technological advantages have forced the United States to expend significant resources in monitoring of foreign nuclear tests. Sophisticated technologies that have evolved about the framework of seismology and geophysics have made significant contributions in satisfying the national requirement to detect, locate, identify and yield-quantify world-wide nuclear detonations. Yet, there is room for improvement using non-seismic methods, particularly in the area of yield estimation. To this end, this study is intended to develop image processing and analysis methodologies for the discrimination and identification of rock types at nuclear test sites. The rationale of this approach is based on the fact that the recorded seismic wave energy resulted from nuclear explosion depends on the following environmental/lithological factors:

(1) the actual yield of the explosion:

(2) depth of the explosion below the surface;

(3) the degree of physcial coupling between the charge and the adjacent medium; and

(4) the geological nature of the median in which the detonation occurs.

Indeed, rock types analysis is the first step in yield estimation.

To accomplish the goal of rock types discriminated at the nuclear test sites, LANDSAT's multispectral data were used. The choice of the LANDSAT imagery is based on the fact that it is capable of providing a world-wide and repetitive coverages and thus a basis for monitoring nuclear test activities.

The thrust of this study is to exploit the digital information of LANDSAT data in the context of texture-tone analysis for such purposes.

The feasibility of the SR&E's image processing system for lithological analysis has been proven in our Phase I effort based on two test sites in Nevada: the Antler Peak Quadrangle, Nevada at the scale of 1:62,500 (ANA1) and the Duffer Peak Quadrangle, Nevada at 1:48,000 (ANA2) as analogs to foreign nuclear test sites. Specifically, the first site (ANA1) was used as a testbed for methodological development; whereas the second site (ANA2) was designed as an analog area for extracting granite regions used in the Phase I studies. To this end, another site was selected from the Willow Springs and Rosamond Quadrangles, California, particularly to possess these properties for testing the generalizability of the developed methologies:

(1) exposure of granite, but not always in high grounds;

(2) existence of contact zones between granite and alluvium;

(3) availability of both general geologic map and a special Quarternary geologic map where information on surficial material is given.

Phase II effort was designed to test the generalizability of the developed methodologies used in Phase I studies. To classify granite versus non-granite regions, two complementary image analysis techniques were employed. For Site 1, first a supervised classification analysis was conducted to delineate granite areas based on manually selected, but digitally pre-processed training sets, and to reject non-granite regions based on a pre-set statistical model/probability level for identifying pixels which are significantly different from the training sets. Second, an unsupervised clustering analysis based on SR&E's Region Growing Texture Clustering algorithm was performed to extract granite areas by region growing from the cores of the granite training sets. The final definition of granite regions can be either based on the

intersection of these two sets of "granite maps," or removing alluvium from the supervised classification map based on the contact zone information given by the unsupervised classification method. For Site 2, the analysis is much more straightforward since a very accurate classification was generated by using our supervised classification methodologies using the same parameters/ variables applied to Site 1.

Section B: A Brief Review of Relevant Literature on Lithologic Analysis with Image Data

Prior to 1972 and the launch of LANDSAT, pioneer work on reflective properties of minerals was accomplished by Hunt and Salisbury at the USAF Cambridge Research Laboratories (1970, 1973). Their study and explanation of reflective/transmission properties of both minerals and rocks in the visible and near-infrared regions serves as a basis for semi-automatic rock discrimination techniques that exploit the spectral (tone) parameters of multi-spectral imagery. Rather than being a simple empirical result, it turns out that minerals and rocks spectral charcteristics are a direct function of the physics and theory associated with crytal-field theory (Burns, 1970), as evidenced from theoretical and laboratory analyses of the rocks and minerals of the moon (McCord, 1968; further McCord, et al, 1972).

Since then, scientists at the U.S. Geological Survey, Jet Propulsion Laboratory and NASA/Goddard Space Flight Center, have attempted to exploit LANDSAT MSS data for rock types analysis as evidenced from Goetz, et al (1973), Goetz, et al (1975), Vincent, et al (1975), Rowan, et al (1976), Rowan, et al (1977), Abrams, et al (1977), and Podwysocki, et al (1977). Recent works by other researchers including Lyon (1977), Lyon, et al (1978), Hunt (1977), and Siegrist et al (1980), also emphasized digital processing of LANDSAT and other types of multispectral scanner data for optimal combination of spectral channels for rock discrimination.

While the majority of the work cited above emphasized rock types analysis and identification with color enhancement techniques with LANDSAT images, our study is devoted exlusively to extracting rock types using the digital information of the LANDSAT MSS data in the context of texture analysis, which has been largely neglected by previous researchers.

Section C. A Brief Review of Texture Measures and Testing of the RADC/Hsu Texture-tone Analysis Algorithms

For years, texture has been recognized as one of the important criteria for identifying objects and scenes by a photointerpreter, along with other variables such as tone, size, shape, associated features, etc. Here texture means the apparent minute pattern of detail of a given area, described ordinarily by these terms: smooth, fine, rough, coarse, and the like. In digital data processing, texture can mean the spatial distributions of tones of the pixels of a given area. Its attributes have to be specified by the investigator--a specific field of study termed texture feature extraction.

Texture analysis is a rather recent but rapidly growing field of inquiry, though its importance relative to visual perception was recognized by Gibson as early as 1950. Over the past 20 years, many texture measures hve been proposed. This body of literature has been reviewed by Rosenfeld in 1975. In general, these measures can be grouped into two categories: Fourier-based (power spectrum) features and statistical features. Furthermore, it has been found that statistical features perform much better than the others (Rosenfeld, 1975).

Haralick (1975) noted further that there have been six basic approaches: autocorrelation functions (Kaizer, 1955), optical transforms (Lendaris and Stanley, 1970), digital transforms (Gramenopoulous, 1973; Hornung and Smith, 1973; Kirvida and Johnson, 1973), edgeness (Rosenfeld and Thurston, 1971) and related measures (Schachter, Lev, Zucker, and Rosenfeld, 1977; Lev, Zucker, and Rosenfeld, 1977), structural elements (Matheron, 1967; Serra, 1973), and spatial dependency probabilities (Haralick et al, 1973), as well as an extended method (Haralick, 1975). In general, Weszka and Rosenfeld (1975) con-

cluded that statistical features perform much better than Fourier-based features.

Texture analysis has also been approached from the human perceptual point of view. Indeed, the human eyes coupled with the brain are very effective in identifying and interpreting imagery patterns. The only drawback is the slowness of data processing using manual operations. Though this system works empirically, the mechanism by which visual detection and recognition is achieved is still largely unknown, as noted by Barlow, Narsimhan, and Rosenfeld (1972) and Julesz (1975). This field of study has been termed psychopietories, as summarized in Lipkin and Rosenfeld (1970).

With respect to texture perception, Whitman Richards (of MIT) has been conducting experiments under the sponsorship of the Advanced Research Projects Agency (1977). He has concluded that most uniform textures can be simulated by three or four variables, provided that three variables contain the basic elemental tokens of the graphic display. His approach to texture perception has employed a "generalized colorimetry" technique analogous to that used so successfully in studying human color vision. Early work on the perception of visual texture using mainly random dots includes that of Pickett (1967), Polit (1976), and Purks and Richards (1977). Perceptually based texture measures have been developed by Mitchell et al (1977), and Hsu (1977). Thus, we see a convergence emerging between human visual processing and machine-oriented image processing methods. As will be discussed below, we have developed a texture analysis system that indeed is capable of integrating visual processing into a machine-oriented image analysis system.

Under the sponsorship of U.S. Air Force/Rome Air Development Center, this author developed a new texture measure with 17 and 23 variables derived from (3 x 3, Model I) and (5 x 5, Model II) windows, respectively (Hsu, 1977). In

the analysis, the window moves from one pixel to another with an overlapping region between two adjacent pixels; and only the center point is classified.

TABLE I

The Texture-Tone Variables of Model I

	Code	Description of computational funds
1.	MEAN	Average
2.	STD	Standard deviation
3.	SKEW	Skewness } the four central moments
4.	KURT	Kurtosis
5.	MDEVN	$\lvert x_i - \bar{x} \rvert / n$, where x_i = tone value of individual pixel, $\bar{x}$ = mean
6.	MPTCON	$\lvert x_i - x_c \rvert / n$, where x_c = tone value of the center point
7.	MPTREL	$(x_c - x_i)/n$
8.	MINCON	$\lvert x_i - x_j \rvert / n$, i and j are adjacent pixels
9.	MINSQR	$(x_i - x_j)^2/n$
10.	M2NCON	$\lvert x_i - x_k \rvert / n$, i and k are second neighbors
11.	M2NSQR	$(x_i - x_k)^2/n$
12.	MADAT1	Mean area above datum 1 (50)
13.	MADAT2	Mean area above datum 2 (100)
14.	MADAT3	Mean area above datum 3 (150)
15.	MBDAT1	Mean area below datum 1 (50)
16.	MBDAT2	Mean area below datum 2 (100)
17.	MBDAT3	Mean area below datum 3 (105)

In Model I, the seventeen texture variables are as follows: (1) through (4) are the four central moments; (5) is the absolute deviation from the mean; (6) is the contrast of the center point from its neighbors; (7) is the mean brightness of the center point relative to its background; (8) is the contrast between adjacent neighbors; (9) is the sum of the squared values of (8); (10) is the contrast between the second neighbors; (11) is the sum of the squared values of (10); and (12) through (17) are the mean area above and below three datum planes having tonal values of 50, 100, and 150, respectively, on a scale of 0 for black and 255 for white. The code names and computational formulas of these 17 variables are given in Table 1.

In Model II, with a (5 x 5) design, in addition to the above 17 variables, three measures are extracted to characterize the oscillatory nature of the scan lines obtained along both the x and y axes of the data matrix; thus, six variables are available for analysis. They are: (1) sum of the contrast values from peak to trough; (2) sum of the distances of peak positions from the origin; and (3) sum of the numbers of peaks and troughs (see Table 2). This means that there are altogether 23 texture variables in Model II.

TABLE 2

Additional Variables in Model II

	Code	Description or Formula
18.	XCONT	(distances from peaks to troughs) along x-axis
19.	XPEAK	(peak positions from the origin) along x-axis
20.	XPANDT	(number of peaks and troughs) along x-axis
21.	YCONT	(distances from peaks to troughs) along y-axis
22.	YPEAK	(peak positions from the origin) along y-axis
23.	YPANDT	(number of peaks and troughs) along y-axis

In our work for the Air Force Office of Scientific Research (Hsu, 1979 and 1980; Hsu and Burright, 1980), we developed and proved the existence of a perceptually-based three-variable texture analysis system with these measurements: (1) average tone, (2) the first neighbor contrast, and (3) mean deviation from the average tone in our Model 1 described earlier.

Section D. A Brief Note on the Testing of the RADC/Hsu Texture Analysis Algorithms for Terrain Analyses

The testing of the effectiveness of the RADC/Hsu texture analysis algorithm has been conducted mainly at The Pennsylvania State University at College Park, Pa., and at the State University of New York at Binghamton in addition to the current research performed at Susquehanna Resources and Environment, Inc.

The Hsu texture measure algorithm was implemented at the Pennsylvania State University (Geophysics Department) by G. Pavlin in 1979; it was documented as "Computer Programs: HSUDRIVE, TEX13 and TEX 2." Several theses have been written at the Pennsylvania State University using the algorithm to discriminate lithologic types with very promising results in arid regions (see Parker, 1980; Ravenhurst, 1980).

At the State University of New York at Binghamton, Kiracofe (1983) went a step further to test its effectiveness for the discrimination of vegetation types in addition to rock types in the Adirondack region of New York State and proved the algorithms are also effective in terrain analyses in both arid and temperate regions.

Finally, we should note that the U.S. Air Force/Rome Air Development Center and the Defense Mapping Agency have implemented these algorithms and used them for both terrain analysis and target cueing for years.

Section E: Summary and Results of the Phase I Effort

1. Tasks Determined for the Phase-I Effort

From a discussion session held among Mr. Best of AFOSR, Col. Lowrey of DARPA, Mr. Rachlin and his colleagues of U.S. Geological Survey, and Dr. Hsu, it was determined that the tasks of Phase I effort should be aimed at answering the following three questions:

1. How well can we map the granite areas versus non-granite regions using our supervised and unsupervised classification methods in the context of texture analysis?

2. What are the factors affecting the classification results--slope, drainage pattern, data used, methodologies utilized?

3. What are the potential contribution of image processing techniques and methodologies towards the discrimination and even identification of rock types using LANDSAT data?

For data analysis, a study area within Duffer Peak Quadrangle, Nevada was selected by Mr. Dempsie of U.S. Geological Survey. Furthermore, based on the geologic map, 22 training sets were selected manually to cover four major rock types: (1) granite, (2) metamorphic, (3) volcanic, and (4) unconsolidated.

2. The Data Set

To remove the shadow effect of the original LANDSAT data, and to extract information from four MSS bands simultaneously, the following data sets are generated.

(1) First, second and third components from the four MSS bands;

(2) Six ratio bands from the four MSS bands: 4/5, 5/6, 6/7, 4/6, 4/7, and 5/7;

(3) The first component map from 4 selected ratio bands.

Therefore, ten derived image data sets are available for analysis in addi-

tion to the original four MSS bands. The location of the training sets with respect to these derived data sets remain the same.

3. Image Processing and Data Analysis Methodologies Utilized

To analyze the relationship between the selected training sets, and to classify the granite areas versus non-granite regions, the following analytical techniques are utilized.

a. Extraction of texture-tone information of the training sets and the entire data set.

Using the texture-tone extraction algorithm, 29 texture-tone-ratio variables have been generated for any given pixel from four multi-spectral bands using (3 x 3) moving grid. They are composed of 4 tone variables, 12 texture variables (3 from each band), 6 ratio variables, and 6 correlation variables.

For data analysis, the analyst is able to select a portion of the following 29 variables:

BRIGHT4	BRIGHT5	BRIGHT6	BRIGHT7	MINCON4	MINCON5
MINCON6	MINCON7	MDEVN4	MDEVN5	MDEVN6	MDEVN7
STDDEV4	STDDEV5	STDDEV6	STDDEV7	MAXLIN	LOGRAT45
LOGRAT46	LOGRAT47	LOGRAT57	LOGRAT57	LOGRAT67	CORR45
CORR46	CORR47	CORR56	CORR57	CORR67	

b. Analysis of the Training Sets

Based upon the selected variables from 29-variable system, typically we use three variables, the training sets will be analyzed and edited so that each training set will meet the following two criteria:

(1) single mode; if two modes exist in one training set, the set will be split into subsets;

(2) extreme outliers are to be removed based on a statistical confidence level.

c. Discriminant Analysis of the Training Sets

After the training sets are edited or preprocessed, they will be analyzed in terms of how close they are between pairs of training sets using the means of selected tone-texture variables. The distance is generally measured by statistical distance calling Mahalanobis D^2 with or without a log-determinant term.

While the D^2 distance is indicative of the degree of similarity and dissimilarity between two training sets, the analyst usually uses a confusion matrix--classification result using only the training sets--to examine how well these training sets are separated. The analyst will then decide whether he should proceed with a classification analysis of the entire test set. In general, if dissimilar training sets are confused, a classification analysis should not be conducted.

d. Supervised Classification Methods

As mentioned earlier, a supervised classification analysis can be made only when the traiing sets are well separated. To achieve this goal, the following steps can be taken:

(1) purify the training sets as in (b);

(2) change the location of the training sets;

(3) increase the power of the feature extractor by using (i) more texture-tone variables, and (ii) using different spectral-band combinations; and

(4) increase the power of the classifier by using a non-Gauseian model if the data are essentially non-multi-variate normal.

In the analysis, we have done all these image processing techniques except step (2), changing the location of the training sets.

e. The Actual Supervised Classification Procedures Applied to the Duffer Peak Quad

Step 1. Four ratio bands (45,56,67,47) were generated as the basis for generating 29 tone-texture-logratio-correlation variables for each pixel.

Step 2. Preprocessing of the manually-selected Training Sets.

As noted training sets were selected as calibration samples of four major rock types. Using information from bands 4/5 and 4/7, these original 22 sets were processed into 25 sets as illustrated in page 13 of the Phase 1 Report. This automated preprocessing technique is designed to purify the training sets by two methods:

1. split a bimodal distribution into two sub-sets; and
2. remove outliers of the distribution from the training sets.

Step 3. Analysis of the Preprocessed Training Sets.

After these 25 derived training sets were generated, we proceeded to analyze the separation pattern among them using only 12 variables from the 29-variable system. These 12 variables are composed of 4 tones and 8 texture measures from 4 spectral bands as follows:

Tone variables are from the 4 spectral bands;

Texture variables are the 1st neighbor contrast and the Mean Deviation measures derived from a (3x3) moving grid from all 4 spectral bands.

The result of a confusion analysis was given in Table 4 of the Phase I Report.

Step 4. Since it was evident from this analysis that the training sets of granite were confused only among themselves except G1, but not with others (see Table 5 of the Phase I Report), we then proceeded to generate only training sets for granite including preprocessing of the sets using G2, G3, G4 and G5 data. (see Table 3)

This step is to set up a supervised classification using only the training sets from granite. The rest of rock types will be treated as rejects using a probability cutoff criterion.

Step 5. After Step 4, we proceeded to generate a classification map using only 7 feature variables in the classifier-4 tone plus 3 texture measures selected from the original 28-variable system as follow:

Brightness 4/5	1st neighbor contrast 5/6
Brightness 5/6	Mean Deviation 4/5
Brightness 6/7	Standard Deviation 6/7 (see Table 4)
Brightness 4/7	

Step 6. Printing of the Decision Map as given in Figure 1 of the Phase I and Phase II Reports.

TABLE 3

Confusion Matrix Showing only the Granite Sets

(Note that G2 through G5 are confused only among themselves)

From Set	G1	G2	G3	G4	G5	Sum
G1	34	2	3	4	3	
	13.18	0.00	0.00	0.00	1.16	
G2	0	1.34	0	38	71	
	0.00	48.20	0.00	13.67	25.54	87
G3	0	0	61	0	1.14	
	0.00	0.00	32.80	0.00	61.29	94
G4	0	13	1	66	56	
	0.00	7.30	0.56	37.08	31.46	76
G5	0	0	1	0	1.61	
	0.00	0.00	0.62	0.00	99.38	100

TABLE 4

The 7-Variable Texture-Tone Analysis System

STEP 1 VARIABLES: BRIGHT4 BRIGHT5 BRIGHT6 BRIGHT7 MINCON5 MDEVN4 STODEV6

Rank of each set:

TRANSTG2 = 7 TRANSTG3 = 7 TRANSTG4 = 7 TRANSTG5 = 7

Confusion Matrix from a Non-Gaussian Classifier

	TRANSTG2	TRANSTG3	TRANSTG4	TRANSTG5
TRANSTG2	211	0	63	5
TRANSTG3	0	164	2	20
TRANSTG4	62	2	113	2
TRANSTG5	12	31	19	102

Total Correct Classification = 73.02 percent.
Actual Correct Classification = 73.02 percent.

This indicates that even granite sets are well separated.

f. The Experimental Results

From three experimental data sets, it can be concluded that:

(1) For rock type analysis, data Set 3 composed of these 4 ratio bands:

4/6, 4/7, 5/7, 6/7 is most effective. Data Set I with the 4 original 4 LANDSAT MSS bands is least affective. Figure 1, a decision map, indicates that the vast majority of granite areas are correctly identifled, except

(a) the granite area, within which the training set GI (which was not used in the analysis is located, is largely classified as non-granite, and

(b) one "metamorphic rock" area as labeled in the geologic map was largely classified as "granite."

These two regions will be investigated further using our unsupervised segmentation algorithm in the next section.

(2) Regarding the classifiers, our non-Guassian classifier with 7 texture-tone variables is superior to the Guassian classifier no matter whether it utilizes 7 or 16 texture-tone variables.

(3) There is little difference between 7-variable Gaussian classifier and 16-variable Gaussian classifier in terms of the confusion matrix using the training sets data.

(4) In terms of correct classification of the granite versus non-granite regions (areal distribution), both our Gaussian and non-Gaussian classifiers achieved a level of over 90 percent hit-rate. The Non-Gaussian Classifier is slightly better than the Gaussian Classifier in these experiments.

g. Feature Extraction with an Unsupervised Training Approach

(1) Experimental Design

The goal of these analyses is to extract homogeneous regions in the study area from various LANDSAT ratio bands using our region-growing texture clustering analysis algorithm. Identification of the granite regions becomes a labeling process using training sets information and other related statistical and terrain characteristics data. It was our intention to use the results from

this unsupervised classification method to investigate the areas of misclassification by the supervised classifier. Seven data sets were used in the analysis.

(2) The Results of the Analyses

By examining the results from the experiments, it was concluded that the results from Log Ratio of Band 4 and Band 7 (Figure 2 of Phase I and II Reports) yielded the best overall result. Using the location of the training sets G1 through G5, the major granite areas were identified, corresponding well to the bedrock regions of granite. Particularly, by comparing the results from this unsupervised classification against the supervised classification, we derived that (1) the rejected granite G1 area can be delineated by the Region algorithm, and (2) the confused area in supervised classification between G2 and G3 can be discriminated as well. Similar to the supervised classifier, the Region algorithm failed to distinguish the bedrock granite from the surficial granite in the are near training set G4. As it was determined in other experiments, this boundary can be detected in the analysis with the data set of log ratio of Band4/Band 6.

h. Classification Analysis by a Combination of Supervised and Unsupervised Training Approaches

From the results given earlier, we used a multiple map overlay analysis to delineate the final granite regions as given in Figure 3 of Phase I and Phase II Reports with the following conclusions:

(1) In the areas where training sets information exists, there is a remarkable correspondence between Figure 1 (supervised classification) and Figure 2 (unsupervised classification);

(2) From a manual editing process, we can place the granite G1 area from Figure 2 onto Figure 1;

(3) The areas of misclassification in Figure 1--

i. region between G2 and G3, and

ii. pixels located outside the boundaries of labeled granite regions of G1, G2, G3, G4, and G5 in the northeast, southeast and southwest quadrangles--

can be removed from Figure 1.

(4) Since there is no information regarding ground truth in the area between the location of G1 and G2, we used the result as given in Figure 1 for granite identification; and

(5) Comparing the results as described above in reference to Figure 3, it can be concluded that an extremely high level of correct classification of granite and non-granite has been achieved. It should be noted that we were able to edit this map further using additional ground truth information and the segmentation results given by other ratio bands.

Section F: The Phase II Effort

1. Tasks Defined.

a. To test generalizability of the developed methodologies.

With the successful results obtained through the Phase I effort, it was determined that the tasks for the Phase II effort should be centered around testing the generalizability of the developed methodologies for rock types discrimination using another test site. To this end, a test site located in the Willow Spring and Rosamond Quadrangles, California, was selected.

During the Phase I effort, both Dr. Smith of AFOSR and Dr. Hsu felt that it is not really proper to use geologic maps as the ground truth to evaluate the ability of the LANDSAT data and the effectiveness of given image analysis techniques for the lithologic analysis despite the fact that it was employed that way in the Phase I analysis as specified by the researchers at U.S. Geological Survey serving as consultants and evaluators of the project. Consequently, a special effort was made to select a site for which both the standard U.S.G.S. geologic map and surficial material map are available in addition to the basic criterion for conducting a generalizability study--comparability between the first test site and the second regarding the general lithologic characteristics and environmental conditions. Based upon the following conditions, the Rosamond, California Site was selected:

(1) Exposure of granite at a much lower ground for testing the effectiveness of the developed texture analysis algorithms on extracting granite where the high-ground, well-exposed bedrock condition does not exist.

This criterion was derived from a general feeling that the success at the Duffer Peak Site can be attributed to the condition of granite: good exposure of the bedrock due to a high-ground location for easier detection by the LANDSAT system.

(2) Availability of a surficial material map for the test site: Quarternary geologic maps were located for several sites in the U.S. where granite can be found. The Rosamond Site was finally determined as the second test site based on another criterion on the similarity in climatic conditions; namely, they are located in arid climatic zones.

b. To evaluate the appropriateness of using the general geologic map as ground truth for LANDSAT data analysis.

Although we were advised by the U.S.G.S. officials serving as advisors and evaluators to our project to use the general geologic maps as the ground truth maps for the study areas, both Dr. Smith and Dr. Hsu could not totally accept this approach based upon the fact that:

(1) The general geologic maps were made according to the interpretation of the field geologist(s) regarding the distribution of the bedrocks; but

(2) the LANDSAT system was designed to detect primarily the surficial material, and thus cannot detect sub-surface material and features although such information can sometimes be inferred from the surficial information.

Hence, the best way to resolve this question (dispute) is to treat the first opinion as a working hypothesis, and test it against

empirical data. With the availability of a Quarternary geologic map for the second test site, it is feasible to carry out this task.

c. To evaluate the contribution of the unsupervised classification method to the extraction of lithologic information.

We concluded from the Phase I effort that both supervised and unsupervised classification methods should be used in mapping lithologic features. Since then, the unsupervised training method was developed further using artificial intelligence approaches by the researchers at Susquehanna Resource & Environment, Inc. Accordingly, a portion of the Duffer Peak test site was used to demonstrate the effectiveness of the new approach. This experiment indeed supports further the conclusion derived from the Phase I effort that a combination of supervised and unsupervised classification approaches are needed to extract lithologic features and related tectonic information.

2. The Data Sets

A frame (256x256) pixels from the Los Angeles, California landsat frame was extracted to represent the second test site located at Rosamond (Quadrangle), California. Since it is determined that the shadow effect of the image data is not significant, the original MSS bands were used as the basis for data analysis. Note that ratio bands served as the basis of data analyses for the Duffer Peak Site because of the presence of shadow effect in the image data.

3. Supervised Classification of the Second Test Site

To test the generalizability of the developed methods, identical procedures used in the phase I effort will be employed to the second test-

site data. The following sections described the methods by which rock types were extracted from the Rosamond Site.

(a) The characteristics of the training sets

As mentioned earlier, we treat the geologic map of the test site as the hypothesized ground truth. Hence, the training sets were selected according to the information given by the geologic map. Figure 4 is a portion of the Willow Spring and Rosamond Quadrangles, California, from which eleven training sets were extracted to represent five rock terrain types as follows:

(i) A1, A2 and A3 for alluvium;

(ii) G1, G2, G3 and G4 for granite;

(iii) S1 for schist;

(iv) T1 and T2 for tuff; and

(v) D1 for drybed.

(b) Generation of 29 texture-tone variables

Follow the same procedure used in the Duffer Peak study; twenty-nine texture-tone variables were generated for each pixel in the (256x256) frame from the form LANDSAT MSS bands based on the original (3x3) moving grid and texture analysis model.

(c) Pre-processing of the training sets

To purify the training sets such that each set is uniform, outliers in each training set (distribution) were removed automatically using information from Band 4 and Band 7. In addition, if a bimodal distribution is found, it will be split into two subsets. Analyses of the training sets indicate that only a few outliers exist in each of the training sets as witnessed from the following data (Table 5).

TABLE 5
Pre-processing of the Framing Sets

Training Set ID	No. of Pixels (original)	No. Pixels after Editing
A1	256	251
A2	256	246
A3	256	242
G1	256	249
G2	256	249
G3	336	324
G4	256	248
S1	208	242
T1	171	168
T2	209	209
D1		

(d) Selection of the best discriminators from the 29-variable system

To determine a subset from a large number of variables as the best discriminators, a stepwise discriminant analysis is generally employed. However, it should be noted that the results of the analysis are highly dependent on the way the discriminant function is set up. For instance, in one case the best discriminator can be designed to discriminate the closest pair of the training sets; on the other, it can be devised to separate training-set classes instead of individual sets in the classes.

Since the goal of this project is to separate granite from alluvium, the step-wise discriminant analysis utilized here follows the second approach--discrimination of classes. The analysis indicates that the best ten variables follows closely with our original concept of texture-tone variables as follows:

(1) Bright 5 (Band 5 tone)

(2) Bright 4

(3) Bright 7

(4) Bright 6

(5) Standard Deviation 6

(6) Mean Deviation 5

(7) 1st Neighbor Contrast 7

(8) Mean Deviation 4

(9) Standard Deviation 5

(10) Mean Deviation 7.

(e) Confusion analyses of the training sets

To determine how well the selected variables can separate the training sets, analyses of the training by means of a confusion matrix is generally used. This is achieved by classification of individual pixels into the mean vectors of the training sets. Table 6 is the confusion matrix from the 10-variable system with a correct classification rate of 99.13 percent. The separation between training sets can also be measured by means of the Mahalanobis distance (D^2) as shown in Table 7.

(f) Classification of the study area (test site)

To be consistent to the procedures used in the Duffer Peak experiment, we used the identical seven feature variables to analyze the traiing sets again, and proceed to classify the entire second test site. These seven variables are:

(1) Bright 4, (2) Bright 5, (3) Bright 6, (4) Bright 7,

(5) 1st Neighbor Contrast 5, (6) Mean Deviation 4, and

(7) Standard Deviation 6.

It turns out that these seven variables is a subset of the 10-variable system derived from the stepwise discriminant analysis. Corresponding to Tables 6 and 7, Table 8 and Table 9 indicate the confusion matrix and the Mahalanobis distance between training sets,

respectively. Note that the hit-rate with respect to the classification of the five rock types is 99 percent.

TABLE 6

Confusion Matrix from the 10-Variable System (SR&E)

	A1	A2	A3	G1	G2	G3	G4	D1	S1	T1	T2
A1	247	0	3	0	1	0	0	0	0	0	0
A2	0	246	0	0	0	0	0	0	0	0	0
A3	15	0	223	0	0	1	0	0	0	3	0
G1	0	0	0	225	5	17	1	0	1	0	0
G2	0	0	7	18	207	0	17	0	0	0	0
G3	0	0	1	70	0	253	0	0	0	0	0
G4	0	0	8	30	54	1	155	0	0	0	0
D1	0	0	0	0	0	0	0	242	0	0	0
S1	0	0	0	0	0	0	0	0	204	1	0
T1	0	0	0	0	0	0	0	0	0	153	15
T2	0	0	0	0	0	0	0	0	0	8	201

Classification = 99.13 percent.

TABLE 7

Mahalanobis distances from Row Set to Column Set from 10-Variable System (SR&E)

	A1	A2	A3	G1	G2	G3	G4	D1	S1	T1	T2
A1	0.0	92.3	10.6	56.4	29.3	62.0	24.9	279.8	195.7	115.7	170.0
A2	67.1	0.0	45.9	53.1	50.3	72.8	44.7	298.8	168.0	275.0	470.6
A3	20.1	48.4	0.0	32.0	17.6	36.2	13.1	178.1	122.1	132.2	252.0
G1	48.3	46.2	28.0	0.0	8.5	3.6	5.1	537.1	32.8	34.6	66.0
G2	53.7	49.1	17.2	14.1	0.0	24.9	2.1	469.5	129.7	149.5	279.8
G3	88.0	57.9	36.5	5.5	35.0	0.0	21.6	629.5	73.3	44.7	82.9
G4	79.5	43.1	14.0	14.8	3.8	30.4	0.0	415.7	200.9	173.1	338.2
D1	431.2	251.9	435.6	466.3	500.1	437.7	468.7	0.0	412.3	634.4	775.1
S1	202.7	58.8	110.6	43.6	88.8	31.7	74.9	349.1	0.0	10.7	22.2
T1	57.8	136.7	31.3	35.4	45.1	36.3	38.2	908.9	67.9	0.0	7.8
T2	55.2	84.9	36.9	31.7	32.1	35.7	29.9	399.4	37.7	5.1	0.0

With such a high hit-rate in the training sets classification, we proceed to classify the entire study based upon these (edited) training sets. The result is given in Figure 4, showing the decision on the distribution of granite and other rock types.

TABLE 8

Confusion Matrix of the Training Sets (Rosamond, California test site)

With a Seven-Variable System

Feature Variables: BRIGHT4 BRIGHT5 BRIGHT6 BRIGHT7 MINCON5 MDEVN4 STDDEV6

Rank of each set:

A2 = 7 A3 = 7 G1 = 7 G2 = 7 G3 = 7

D1 = 7 S1 = 7 T1 = 7 T2 = 7

	A1	A2	A3	G1	G2	G3	G4	D1	S1	T1	T2
A1	243	0	6	1	0	0	1	0	0	0	0
A2	0	246	0	0	0	0	0	0	0	0	0
A3	19	1	0	2	0	0	0	0	0	3	0
G1	0	0	1	225	3	17	2	0	1	0	0
G2	0	0	8	26	194	0	21	0	0	0	0
G3	0	0	0	82	0	239	2	0	0	1	0
G4	0	0	7	30	50	2	159	0	0	0	0
D1	0	0	0	0	0	0	0	242	0	0	0
S1	0	0	0	0	0	0	0	0	203	2	0
T1	0	0	0	0	0	0	0	0	2	149	17
T2	0	0	0	0	0	0	0	0	0	11	198

Classification = 99 percent with respect to five rock types

TABLE 9

The Mahalanobis Distance Between the Training Sets from the 7-Variable Systems

	A1	A2	A3	G1	G2	G3	G4	D1	S1	T1	T2
A1	0.0	91.9	10.1	54.7	27.0	57.8	22.8	290.3	195.6	113.4	161.1
A2	60.6	0.0	42.4	51.7	44.9	71.5	40.4	284.7	168.4	276.4	467.1
A3	16.8	46.9	0.0	31.9	17.7	35.6	12.9	169.7	115.6	113.2	208.5
G1	46.5	43.0	24.8	0.0	8.1	3.6	5.3	525.1	33.2	30.1	60.2
G2	51.9	47.7	15.9	13.0	0.0	24.7	2.1	461.2	128.4	148.0	272.4
G3	86.6	54.8	36.2	5.0	33.4	0.0	20.8	602.8	72.2	38.1	70.2
G4	74.0	40.1	12.6	14.6	3.6	29.3	0.0	395.7	200.8	174.1	334.0
D1	411.6	240.1	412.8	439.1	478.0	419.9	448.9	0.0	383.1	582.5	717.6
S1	193.1	56.6	104.7	38.4	82.1	29.2	68.2	341.7	0.0	9.8	22.5
T1	49.5	137.1	28.2	35.5	38.1	37.4	35.7	832.6	63.0	0.0	6.5
T2	52.3	84.7	34.5	31.6	32.0	35.1	29.7	394.9	37.4	5.2	0.0

4. Discussions on the Correspondence Between the Decision Map from the LANDSAT Data and the General Geologic Map and the Quarternary Geologic Map, Respectively.

Since the goal of our lithologic analysis is to separate granite from non-granite regions, we will concentrate our analyses on the distribution of granite in the decision map against that delineated in (1) the geologic map, and (2) the Quarternary geologic map as follows.

a. A comparison against the 1943 geologic map

To provide a basis for comparative analyses, a (10x10) grid was

constructed for the study area. Figure 5 is a portion of the Willow Spring and Rosamond Quadrangles, California; the granite region was located in cells along rows #4, #5, #6, #7 and #8. Alluvium is located mainly on the northern side of the granite region.

Figure 6 is the decision map derived from the LANDSAT data based on the above-discussed training sets and image processing methods. For a better display; it is broken up into three portions with Figure 6a showing the granite region at the middle portion of the map, and Figure 6b and Figure 6c indicating the upper and lower segments of the classification results, respectively. In addition, the outline of the granite regoin from Figure 5 was traced onto Figure 6 for an easier visual analysis.

In general, the computer decision map (Figure 6a) corresponds rather well to the geologic map in terms of the distribution of granite. Discrepancy between them occurs mainly at three subregions:

(1) Cells #(6,2), (6,3), (6,4), and (7.4);

(2) Cells #(4,7), (4.8), (4,9), (4.10); and

(3) Cells #(8,8), (8,9), and (8,10).

In case (1), those cells were designated as granite in the geologic map; whereas, they are classified essentially as alluvium.

In case (2), a versed pattern of case (1) is witnessed.

Case (3) is similar to case (1) with a less degree of discrepancy.

b. A comparison against the Quarternary geologic map

(1) Note on characteristics of the Quarternary Geologic Map.

The Quarternary Geologic Map of the study area was made by researchers (D.J. Ponti, D.B. Burke, and C.W. Hedel) of U.S.G.S.

in 1981, documented as Open-File Report 81-737, and entitled "Map Showing Quarternary Geology of the Central Antelope Valley and Vicinity, California." Along with the map, "discussion" and "explanation" sections were given to help readers understand how the map was compiled from field work, aerial photos, soil surveys, and other source material, which included nineteen references. The discussion section is given in Appendix 1.

The researchers noted that: "all the upper Quarternary map units are unconsolidated, they have similar, primarily granitic, clast lithologies, and they remain some or all of their original depositional surfaces. These characteristics distinguish the deposits from older Quarternary and pre-Quarternary formations of diverse lithology which are weakly to firmly consolidated and deformed and which preserve none of their original depositional surfaces."

From this explanation, we should treat upper-Quarternary depositional material the same as its parent material in the image data because it still maintains the original characteristics of the bedrock lithology. Since eight layers of Quarternary datings were used to differentiate the relative ages of the material, it is fairly easy for the users to understand which map units belong to Upper Quarternary, and which is Lower Quarternary. In addition, each map unit is described in detail regarding the characteristics of stratification, degree of consolidation, grain size, and other morphological and locational information. We have to conclude that this map is much more appropriate for serving as the ground truth information for the LANDSAT imagery of the study area.

(2) A comparison between the LANDSAT decision map and the quarternary geologic map.

First, we should note that the Quarternary geologic map covers only a portion of the study area; fortunately, the major portion of the granite region is included as given in Figure 7, and referenced by the same (10x10) grid. For an easier, comparative analysis, the bedrock granite was retraced with a dark line. Now let us compare Figure 6a against Figure 7 in terms of the three cases of discrepancies noted between the computer decision and the general (1943) geologic map as follows.

Case 1. In Cells #(6,2) and (6,3), there is a close correspondence between these two maps. This clearly indicates that the (1943) geologic map did not indicate the surficial material of that locale, which is composed of sand dunes (Qds).

Cells #(6,3) and (7,3) were classified as alluvium. The 1981 Quarternary geologic map shows that the area has been highly altered by human actions via construction of transportation routes such as highways and railroads. Therefore, it is difficult to assess that the original granitic material still exists today and can be detected by LANDSAT.

Case 2. The northern border of granite in the Quarternary geologic map along row 4 is located further north as compared to the 1943 geologic map because it encompassed the upper Quarternary deposits (Q6m). This boundary actually corresponds well with the decision map of the LANDSAT data.

Case 3. The material in the upper portion of Cells #(8,8), (8,9), and (8,10) were classified as alluvium by the LANDSAT data. It was mapped by the 1943 geologic map as "granite." In the Quaternary geologic map it was mapped as non-granite bedrock (or outside gr m). However, a proper labeling cannot be determined. A field check is needed to determine the precise characteristics of the material at this location.

5. Conclusions

From the analyses given in previous sections, we have derived the following conclusions:

a. Our developed texture analysis algorithms are indeed generalizable in terms of their effectiveness in extracting granite versus non-granite lithologic features in arid regions.

b. Analyses from the second test site clearly demonstrate that Quarternary geologic maps are much more appropriate than the general geologic maps for serving as "ground truth" to the LANDSAT image data. Although it is desirable to extract bedrock information from the LANDSAT image data, it is definitely not correct to conclude that the LANDSAT data are not effective when the classification map (based on the image data and a certain set of image analysis algorithms) cannot match perfectly to the general geologic map regarding the distribution of lithologic (bedrock) features.

c. The success of our experiments may be attributed to three image analysis alorithms that are not generally available to other researchers:

(1) "Training set pre-processor" for purifying the training set data so that each set is uniform internally.

(2) "Non-Gaussian Classifier" for improving the classification result when the training sets data are not really normally distributed.

(3) "Region Growing Texture Clustering Algorithm" for processing the image data in an unsupervised training classification mode. This algorithm is capable of detecting the contact zone between granite and alluvium regions, and thus extracting the feature according to an additional parameter--spatial characteristics of the interaction among lithologic units. Although this algorithm was not needed for the analyses of the Rosamond, California test site, it was necessary for editing out "granite pixels" that are distributed beyond the limit of the granite boundaries in the Duffer Peak, Nevada test site.

With newly developed capability in the "Region" algorithm, we will demonstrate its ability to extract alluvium including the contact zones.

Section G: The Duffer Peak Site Revisited

1. Introduction

In our Phase I effort, we employed an iterative scene segmentation algorithm to depict the evolutionary patterns of the imagery structures of the study area, starting from each pixel as a group, and ending with a few thousand groups in the (256x256=65,536) frame. Since the grouping distances are designed to progress linearly with an even increment of one unit from one iteration to the next, interior pixels are grouped first, and the boundary pixels (having a larger neighbor contrast) should remain distinctive for a while during the continuous grouping process, revealing the contact zone between two lithologic units.

To a certain degree, we were successful in identifying granite pixels (from the supervised classification) that should be removed from the original decision map because they were located beyond the "contact zones." Nevertheless, we now feel that a better algorithm can be employed to identify the contact zone directly, instead of relying on a continuous, iterative segmentation process, the original region algorithm. The new algorithm is called "Edge" algorithm because it defines feature edge (versus spurious edge) according to certain spatial characteristics corresponding to the physical properties of modeled features. And from these feature edges, we should be able to extract the alluvium first because the particles of alluvium are much more uniform than those of granite, and the contact zone between granite and alluvium should be stronger than the internal edges of alluvium.

2. Demonstration of the Capability of "Edge" Algorithm.

For this experiment, only the NW quarter of Figure 1 (Decision map from the supervised classification) will be used in view of the fact that it represents the major area of misclassification by the supervised method due to the

inability of the supervised method to detect the contact zone. Note that a supervised classification approach is essentially an aspatial processor. Now we present Figure 1 again as Figure 8 with the contact zones marked by thicker lines. For better discussions, the NW Quarter is subdivided further into the four sections as indicated in Figure 8; and we will concentrate our analyses in the lower half of the test area, particularly the SE cell, where alluvium is located.

Let us recall that the bedrock boundary and the granite regions are marked by "diagonal strikes," the numerals are classfied granite pixels and "blanks" are non-granite areas.

With respect to the SE cell of the NE quarter of Figure 8, it is essentially a non-granite country according to the geologic map; however, a major portion of that cell was classified as "granite" according to the LANDSAT data and our algorithms. Without field work, it is difficult to conclude which decision is right. It is entirely possible that they are alluvium in terms of the grain size particles, but they were possibly derived from the parent material (granite) situated at higher grounds.

We will attempt to answer the above question particularly by means of a decision map generated by our "Edge" algorithm. Particularly, we would like to point out that the decision map was derived by using a two-band simultaneous segmentation method: the first band is represented by the first component scores of the original four MSS bands, and the second band is the ratio between Band 4 and Band 7. The result is shown in Figure 9 (a region map) and Figure 10 (an edge map of Figure 9).

By comparing Figure 9 against NW Quad. of Figure 7 (classification map with a supervised classification method), we can immediately notice that the contact zone between the granite unit and the alluvium area (as indicated in

the geologic map) was clearly detected by the Edge Algorithm with a very high degree of accuracy. In addition, the alluvium area was determined as one uniform region, whereas the granite area was determined as a composition of a great number of highly texturalized local features. This phenomenon corresponds closely to our earlier prediction that finer particles would group together sooner than coarser particles.

From the decision map of Figure 9, we can conclude that the particles in the SE quarter of Figure 9 and its continguous part in the NE and SW quarter are finer than those in the rest of the study area particularly the NW quarter. However, it is difficult to conclude that the pixels in the SE quarter are definitely alluvium in the general sense of lithologic classification. From the terrain data, it is entirely possible that those fine particles were derived from the parent material called granite. If those materials are of upper Quarternary period, they could still maintain the property of the parent rock. Yet, one thing is sure: the contact zone between granite and non-granite is still detectable by the two-band simultaneous segmentation meth d of our "Edge" algorithms. This contact zone is clearly shown in Figure 10, the edge version of Figure 9.

Section H: General Conclusions

From Phase I and Phase II research efforts on rock types analysis with LANDSAT MSS data and our texture analysis algorithms, we have come a long way on the understanding of the interaction between lithologic material with the LANDSAT sensing system on one level, and the spatial interaction among individual pixels and groups of pixels on another. Only from these two aspects of "vertical-and-horizontal" interactions, would we have a better handle on rock types discrimination and identification with remote sensing technologies and methodologies.

At the beginning of this project, we were told that no one in the U.S. in the past twenty years had been able to correctly extract granite versus non-granite from the Duffer Peak test site. As demonstrated in this technical report, researchers at SR&E have accomplished the task that has been extremely difficult for other researchers to handle. We would like to share our thoughts with scientists having interests in lithologic analyses with image data on what we have learned from these experiments as follows.

1. Technical advisors and evaluators to our project have insisted on using the general geologic maps as "ground truth" information for the corresponding image data because in many cases they are the best available material to the research. We consider this position as too rigid; and properly, geologic maps should be treated as one of the many information sources for obtaining real ground truth that can be detected by the sensors.

2. It is a well-known fact that the characteristics of training sets affect significantly the final classification results. However, in the past, it was difficult to pre-process the training set automatically with sophisticated algorithms because of hardware limitations, such as not

enough core capacity to perform clustering analyses. Our success at the Duffer Peak site can be partially attributed to good training sets after they were pre-processed.

3. The final classification results can also be affected by the mathematical model that the classifier uses. If the training sets data are Gaussian, the Gaussian model is the best; if not, other models based on non-parametric distributions are better than a Gaussian model. In the past and even today, the majority of researchers are still using Gaussian model for the classifier because it is easy to program, or readily available. However, if the data are not Gaussian even after pre-processing, you most likely will increase the error rate by five to ten percent in the decision map. This is precisely the case for the Duffer Peak site: Our non-Gaussian classifier is capable of removing a substantial amount of "granite" pixels in the non-granite area that are present in the decision map generated by a Gaussian classifier.

With respect to the Rosamond, California test site, both the Gaussian and the non-Gaussian classifiers produced the same result. Thus, either model is acceptable.

4. Future research efforts should be centered around developing unsupervised classification methods for extracting lithologic features. As demonstrated in this project, this approach can be effectively used in conjunction with a well-designed supervised classification to determine the contact zones among various lithologic units, and thus remove the errors made by the classifiers based on the supervised training method.

These unsupervised classification methods can be developed into smart algorithms once certain decision rules are implemented into the feature extraction processes. Artificial intelligence can therefore play an important role in the next phase or generation of image exploitation.

gure 1

Classification Map of Granite Regions, Supervised Method, Non-Gaussian, Ratio Bands: 4/6, 4/7, 5/7, 6/7.

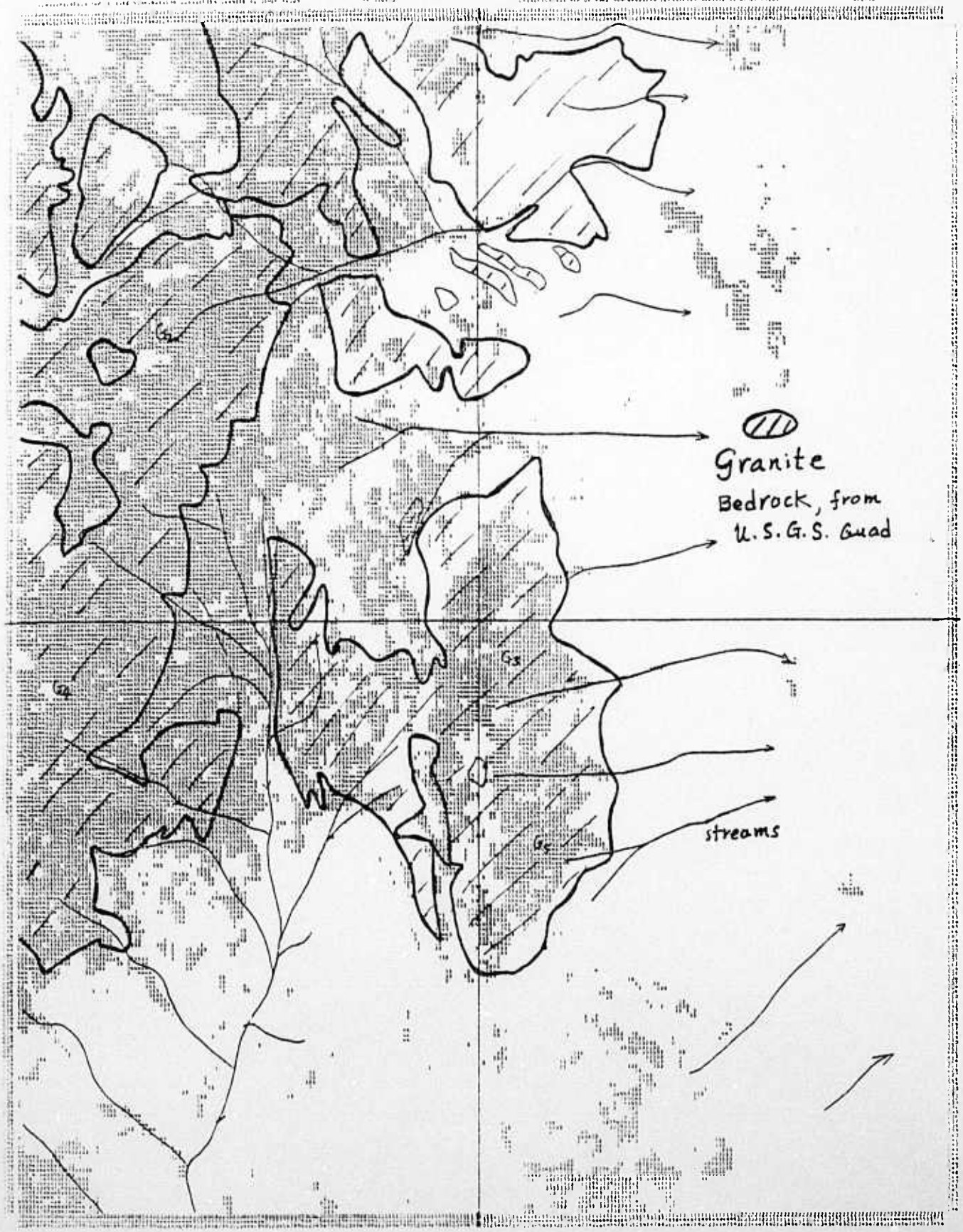

Figure 2:

Dynamic Regions of Granite by Unsupervised Classification Method

Based on Log ratio of Band 4 / Band 7

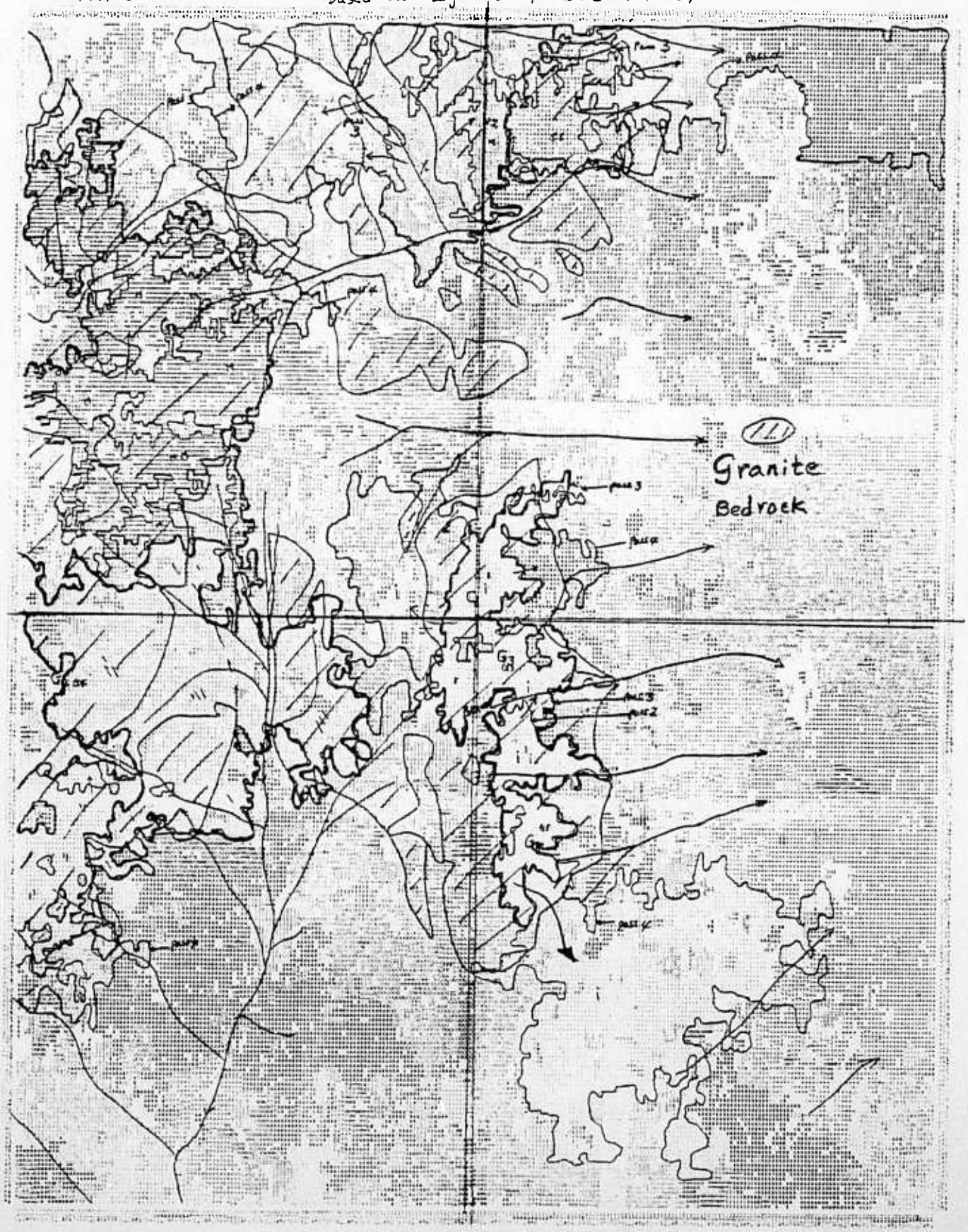

Figur 3. Overlay of Figure 1 and Figure 2: A Final Decision Map

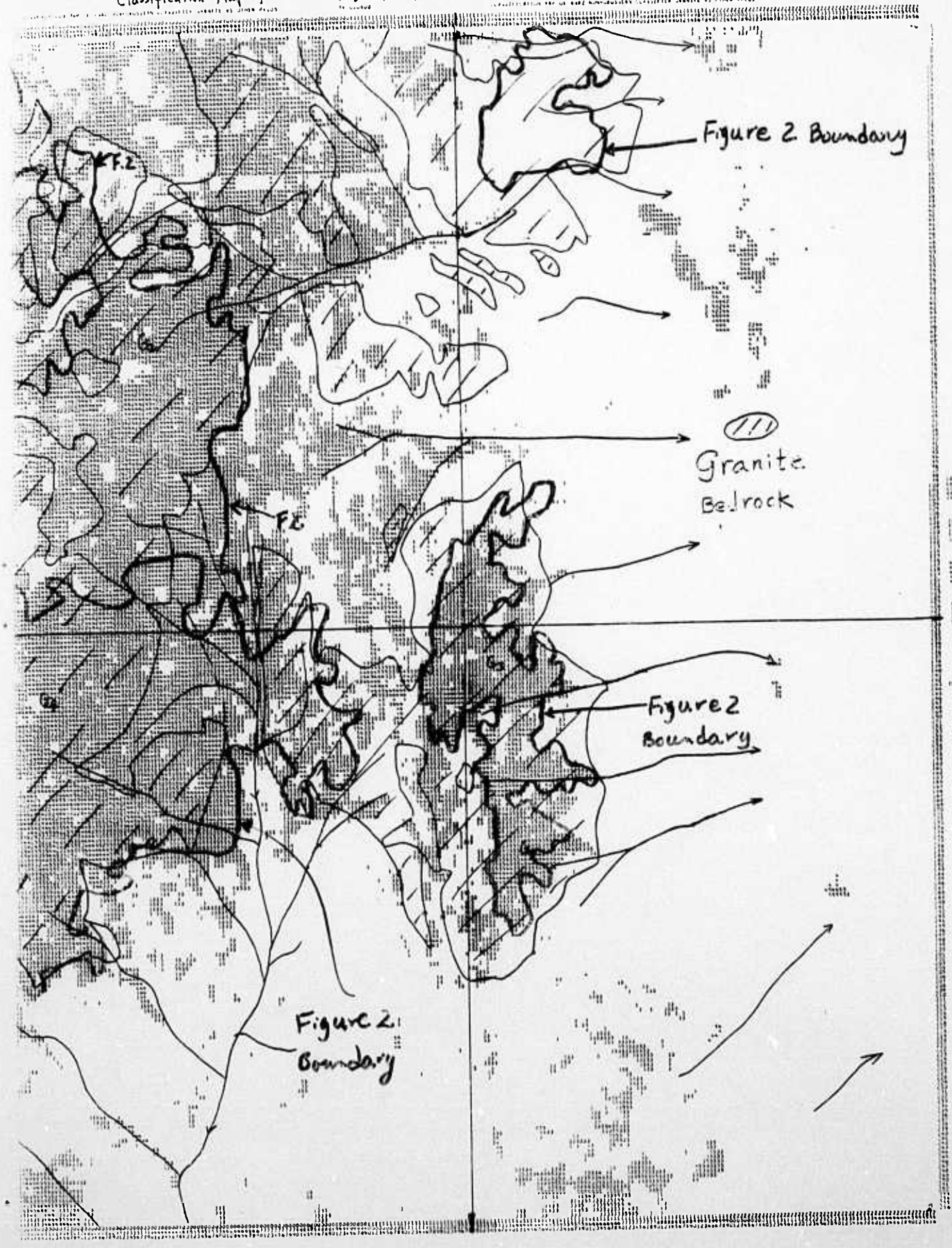

Figure 4. The 1943 Geologic Map of the Study Area with Training Sets Location

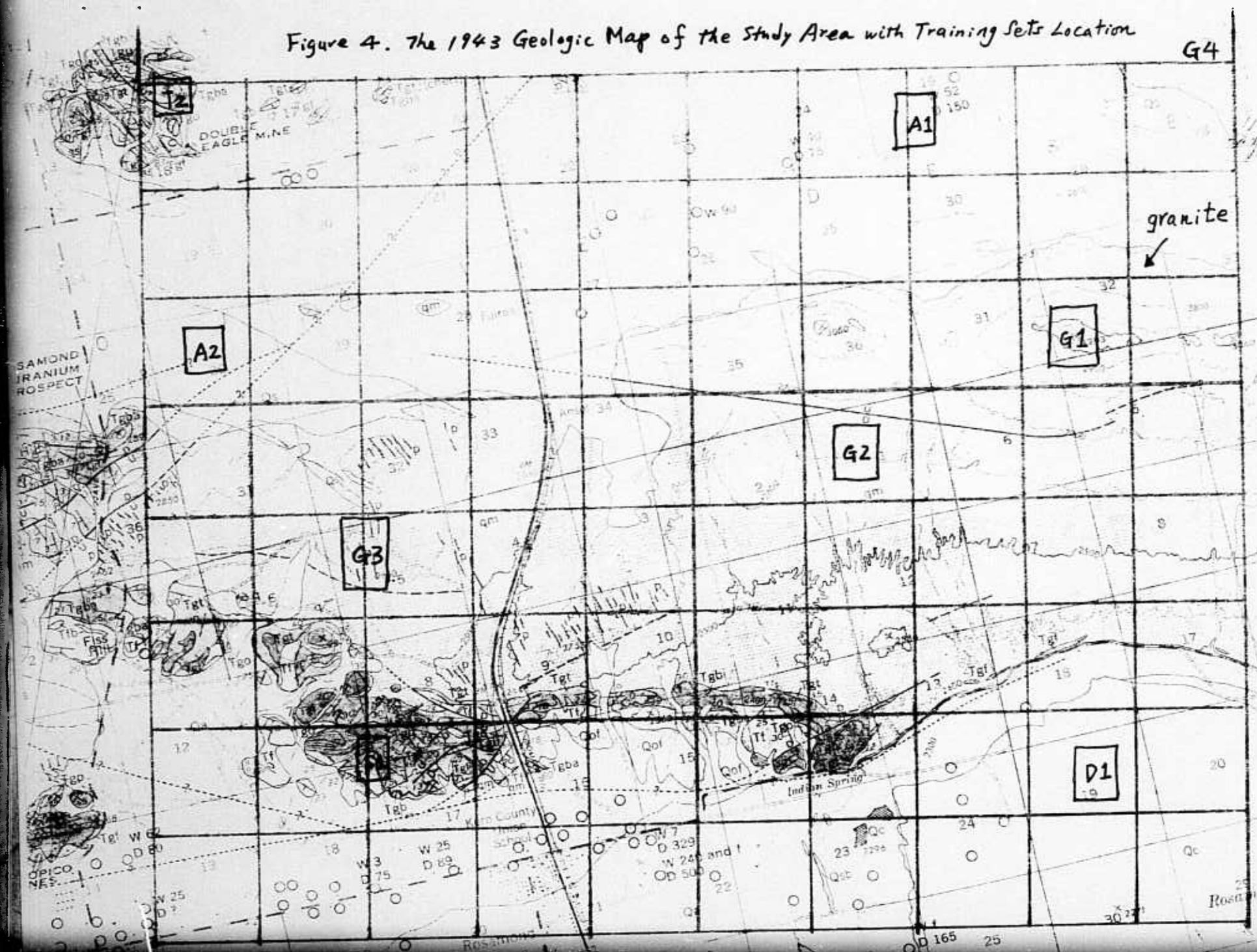

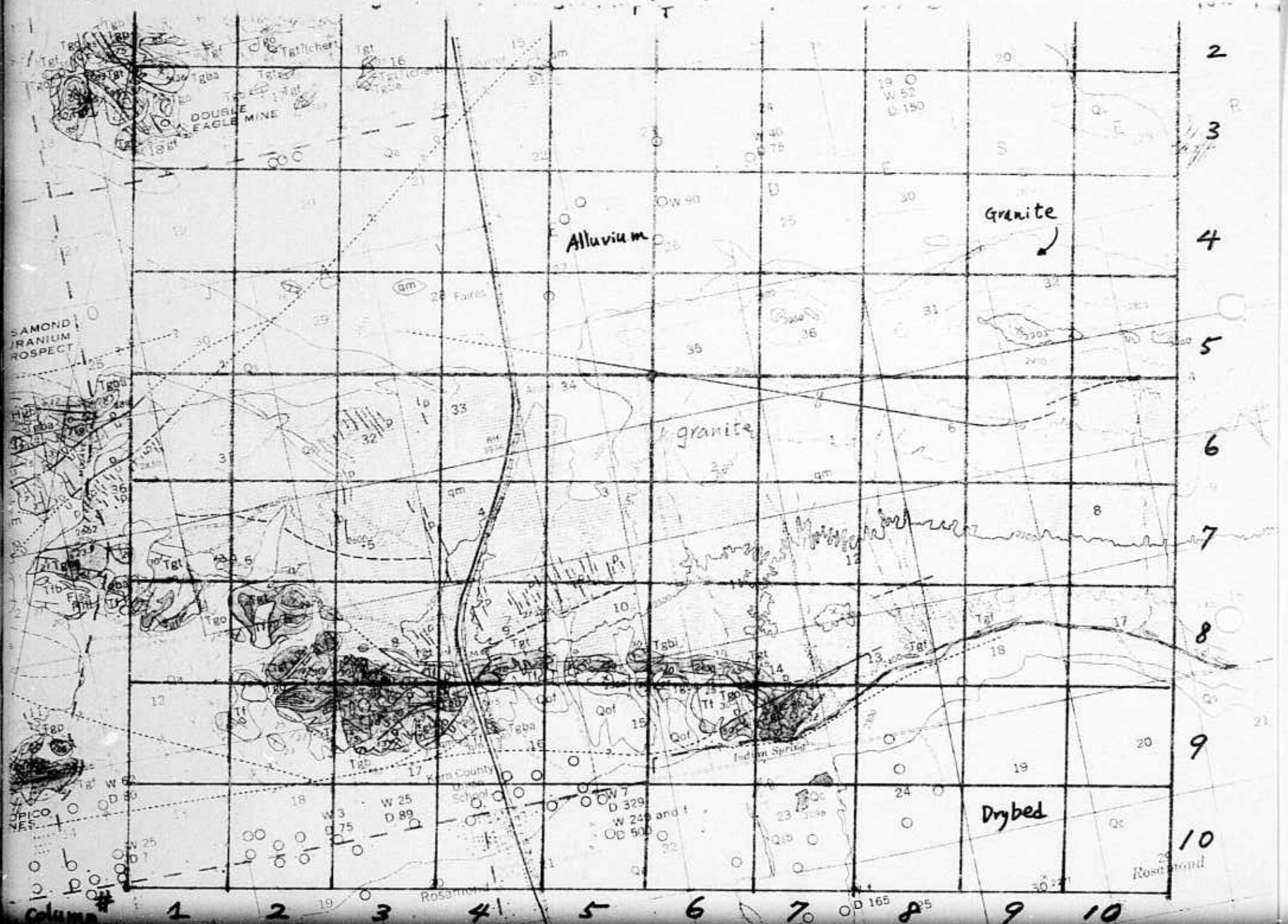
Alluvium
Granite
granite
Drybed
DOUBLE EAGLE MINE
SAMOND URANIUM ROSPECT
Indian Springs
Kern County Union School
Rosamond
Rosamond
Columns
1
2
3
4
5
6
7
8
9
10

Figure 6 Classification Map with LANDSAT Data Using Supervised Method

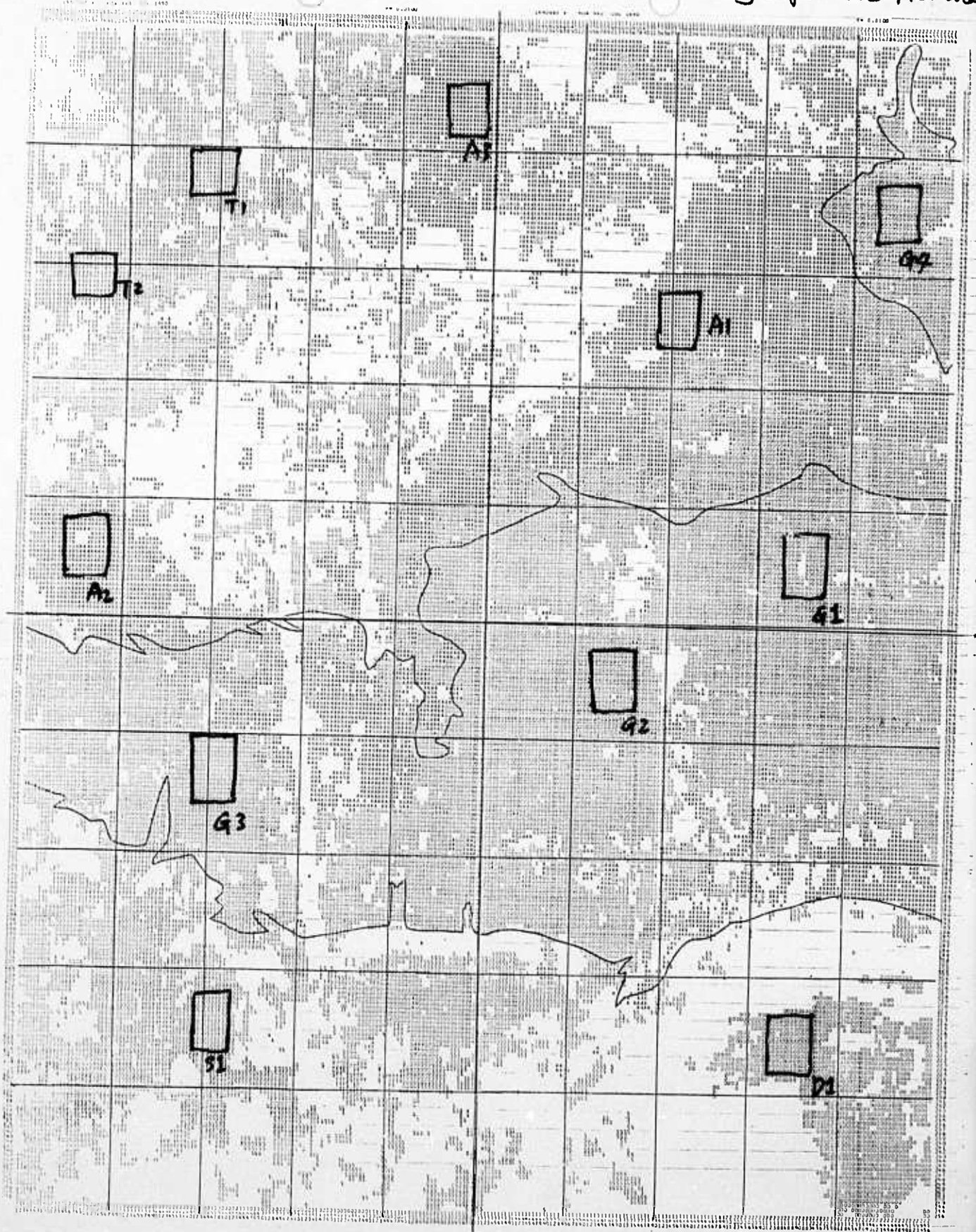

Key: G: granite
A = Alluvium
S = schist
T = Tuff
D = Diabase

Granite Boundary as indicated in the 1965 geology map

Figure 6a. Decision Map from LANDSAT Data (Middle Portion)

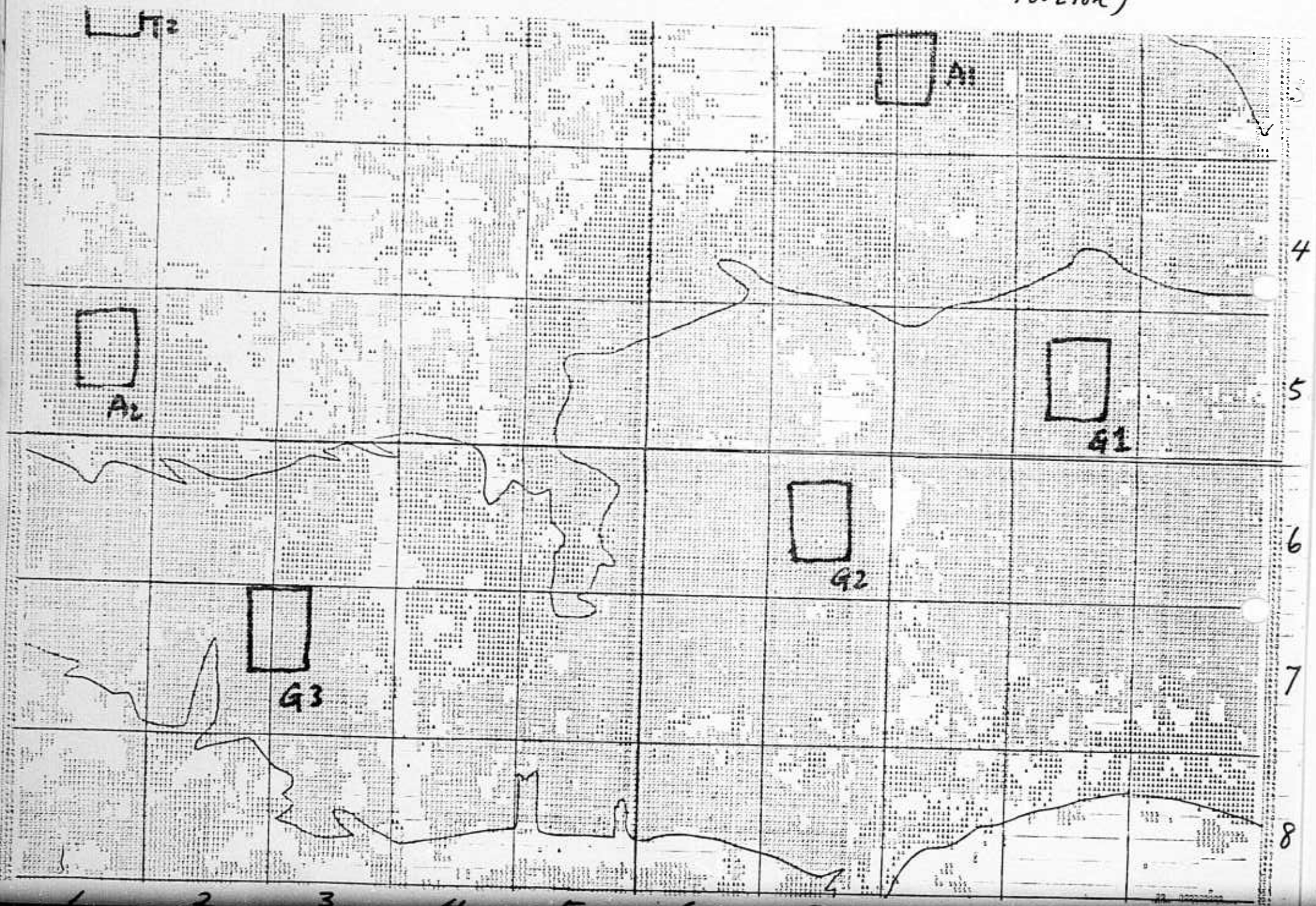

Figure 6 b. Decision Map from LANDSAT Data
(Upper Portion)

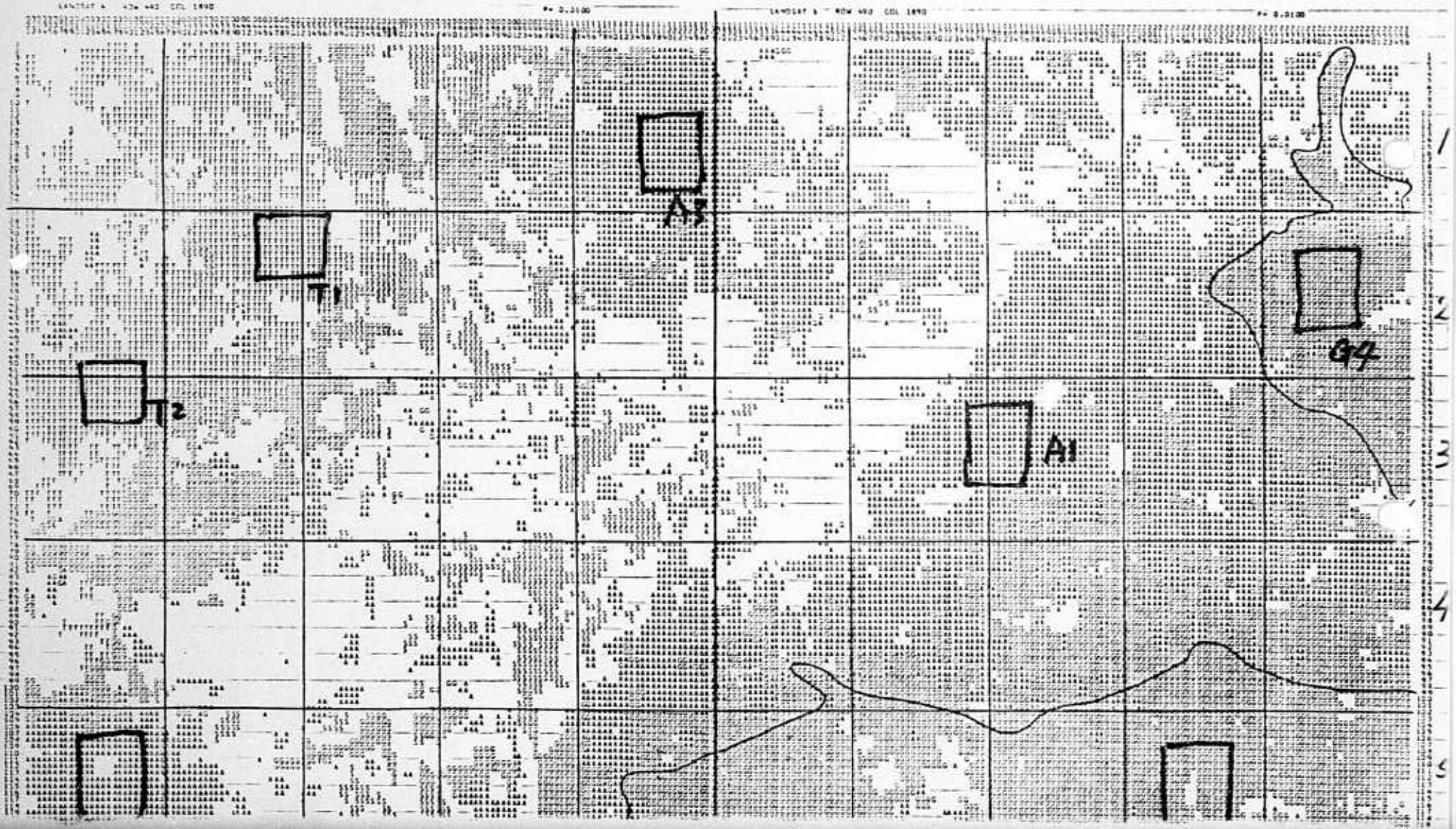

Figure 6c. Decision Map from LANDSAT Data (Lower Portion)

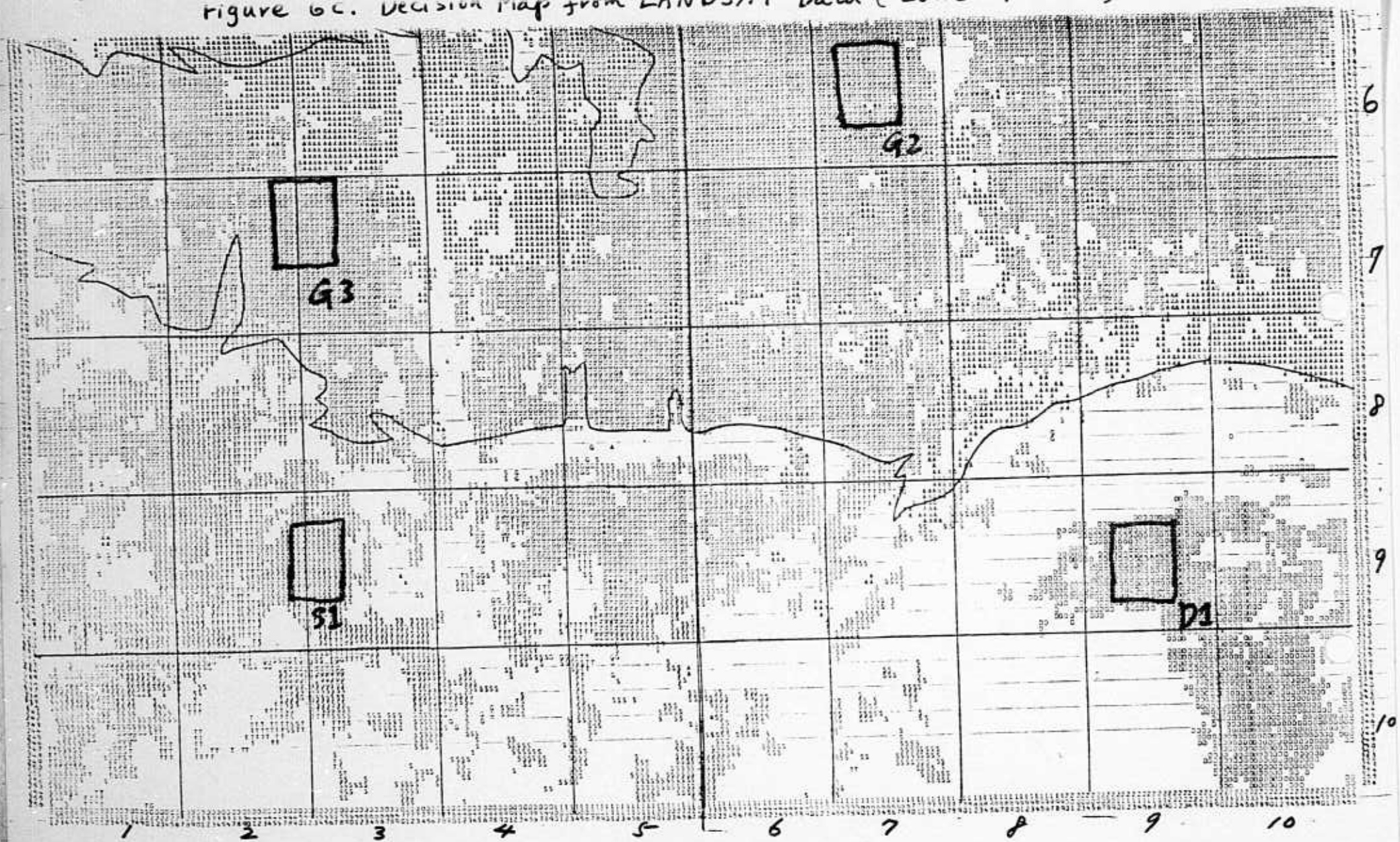

Key: G = Granite
A = Alluvium
S = Schist
Granite Boundary as indicated in the 1943 Geologic Map

Figure 7. The Quarternary Geologic Map of the Study Area
(Open-file Report, 81-737, USGS)

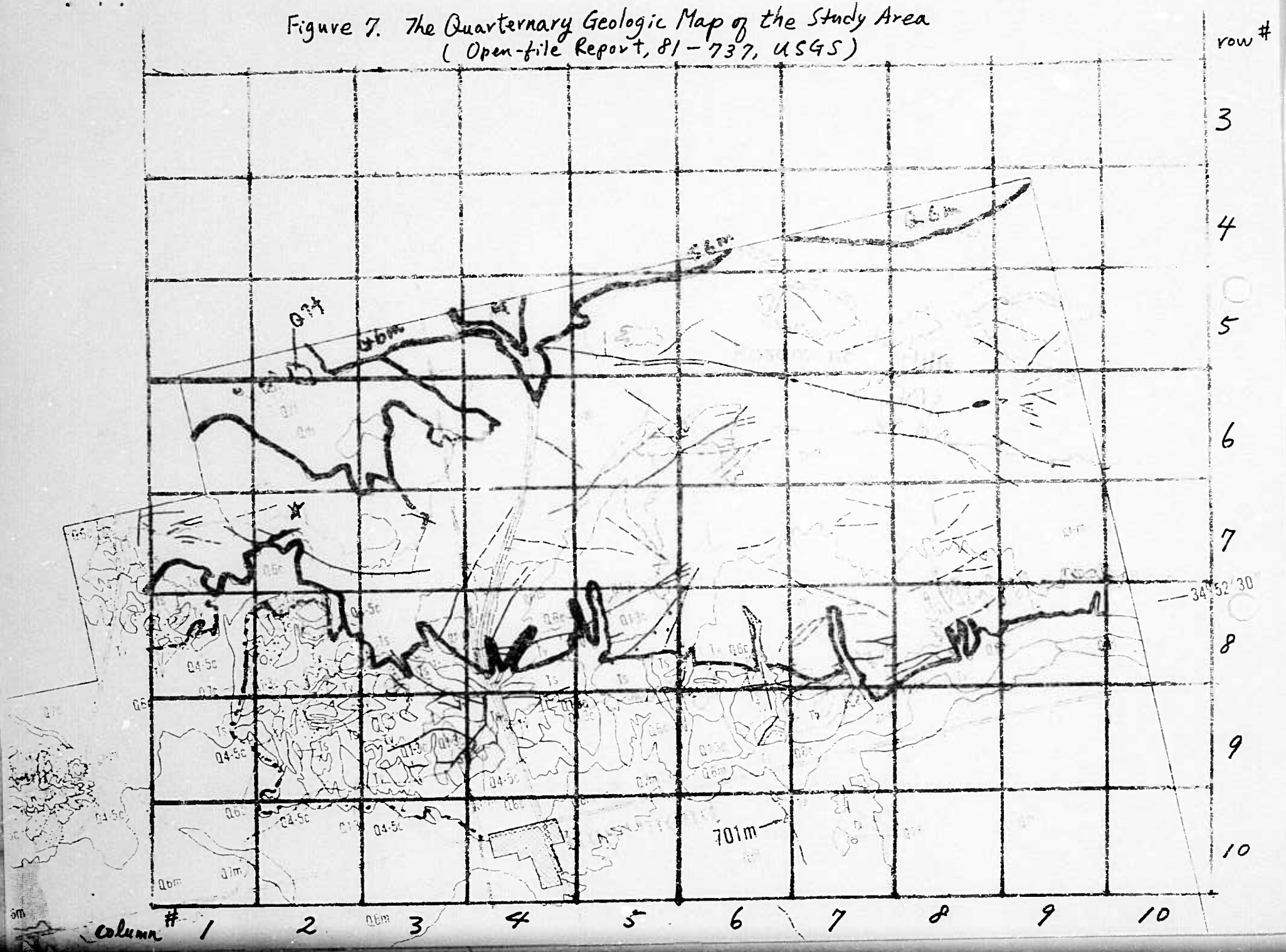

Figure 8 Duffer Peak Quad., Nevada

Classification Map of Granite Regions, Supervised Method, Non-Gaussian, Ratio Bands: 4/6, 4/7, 5/7, 6/7.

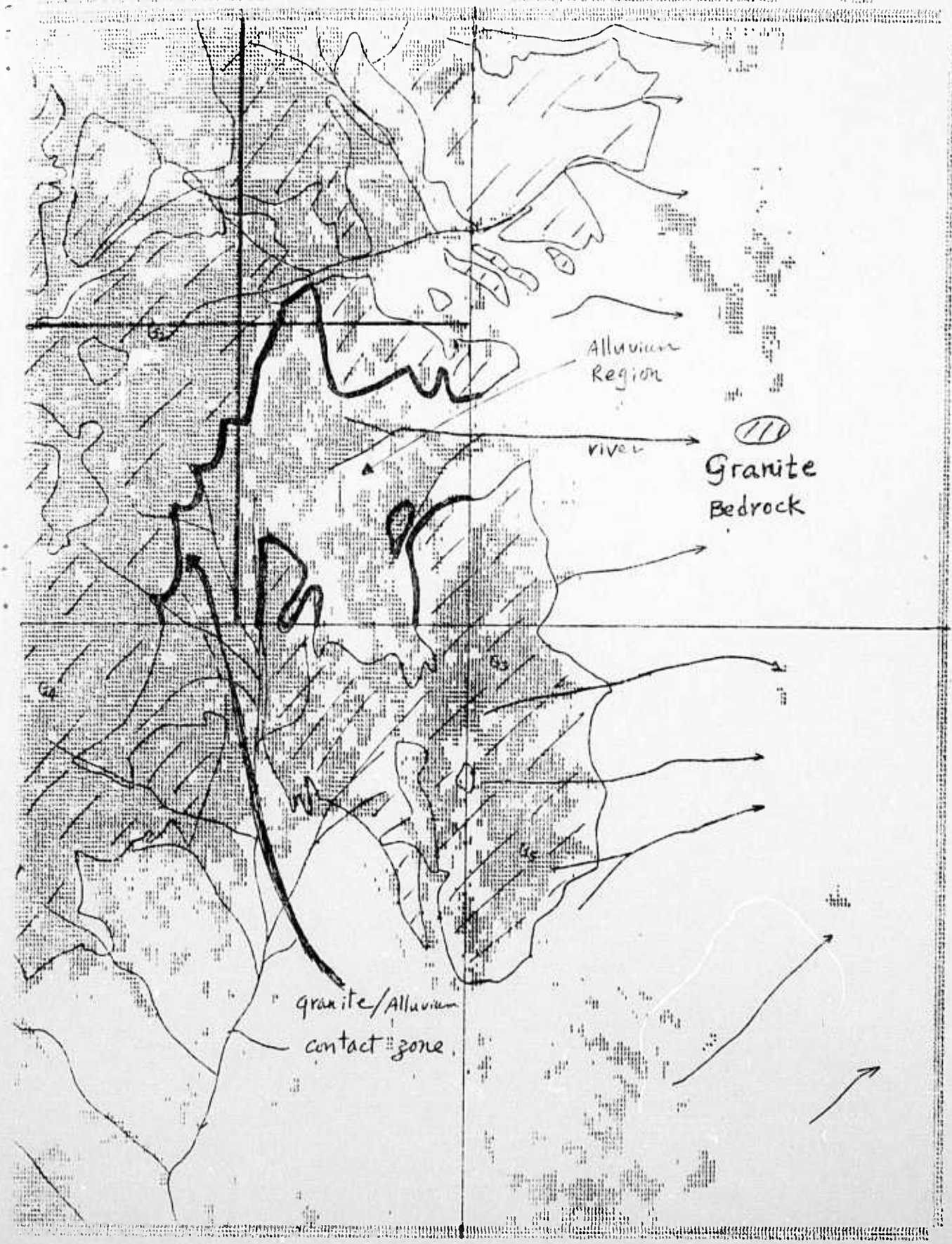

Figure 9 NW Quad. of Fig. 7: Decision M by "Edge"
A Region Map Presentation

A2B9F3(7,12,20) & A2R9TF3(5,10,15)

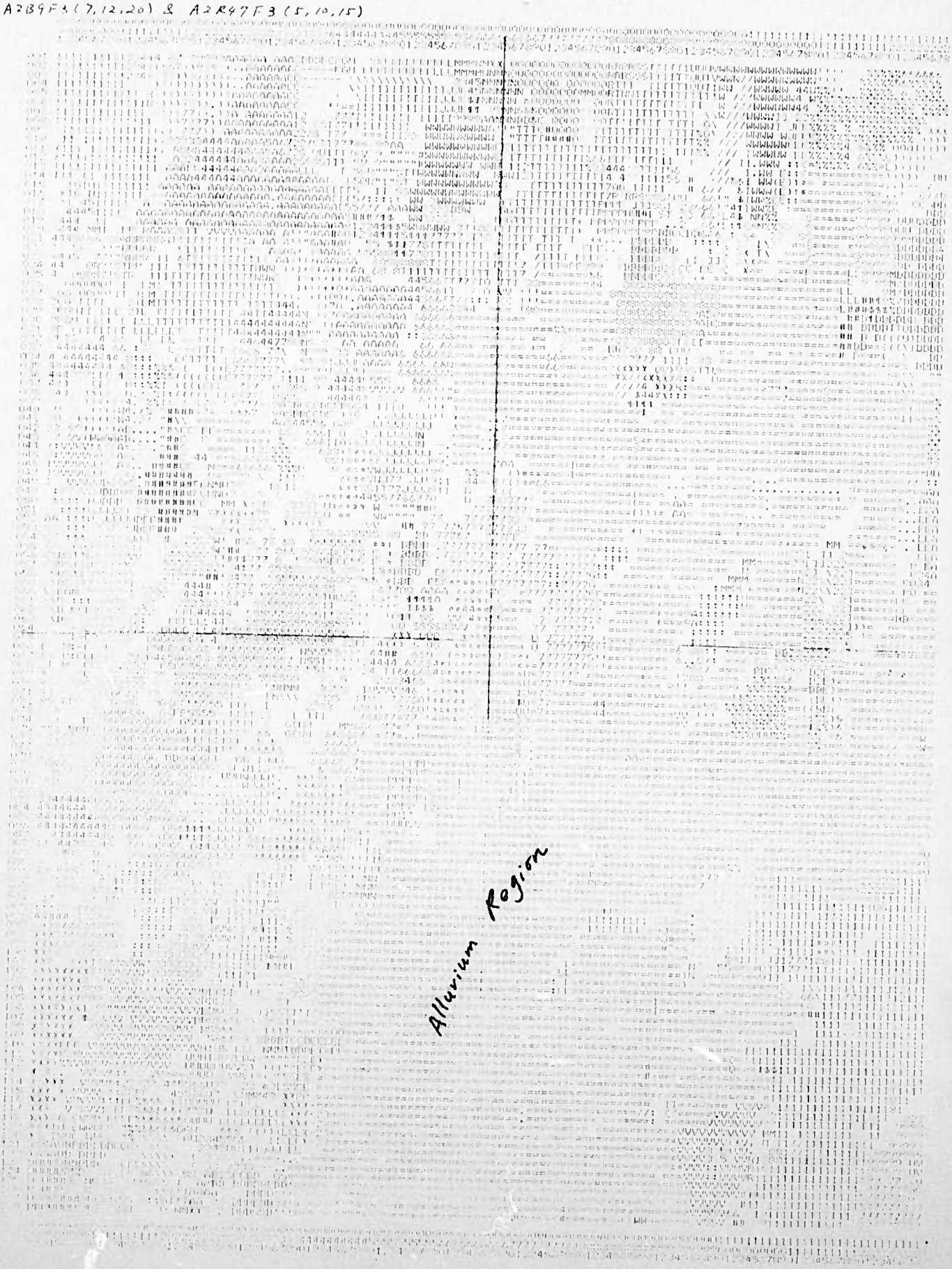

Figure 10 NW Quad. of Figure 7
Decision Map by "Edge"

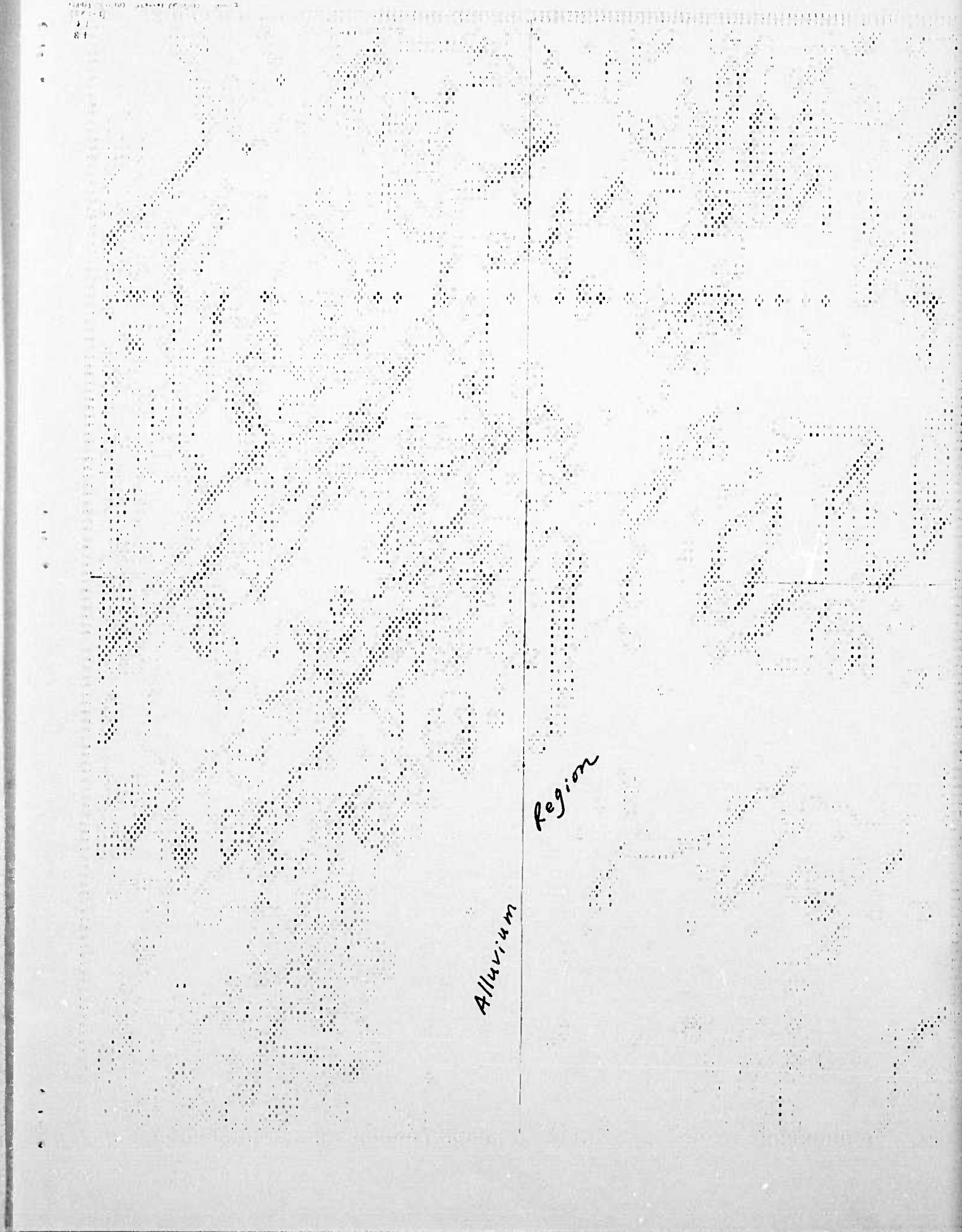

REFERENCES

Abrams, Michael J. "Lithological Mapping," Remotesensing in Geology, Siegal, Barry, and Gillespie, Alan R. (eds.), John Wiley and Sons, New York, 1980, pp. 381-418.

Barlow, H.M., Narasimhan, R. and A. Rosenfeld, "Visual Pattern Analysis in Machines and Animals," Science, 177, 1972, pp. 567-575.

Burns, R.G., Mineralogical Applications of Crystal Field Theory. Camgridge: Cambridge University Press, 1970.

Dahlman, O. and H. Isrealson, Monotoring Undergraound Nuclear Explosions, New York: Elsevier Scientific Publishing Co., 1977.

Gibson, J.J., The Perception of the visual World, New York: Houghton Mifflin, 1950.

Goetz, A.F.H. and F.C.Billingsley, "Digital Image Enhancement Techniques Used in Some ERTS Applications," Contributions to Geology, Vol. 12, No. 2 (Editted by R.B. Parker), Laramie, Wyoming: University of Wyoming, 1973.

Goetz, A.F.H., Billingsley, F.C., Gillespie, A.R., Abrams, M.J., Squires, R.L., Shoemaker, E.M., Lucchitta, I., and D.P. Elston, "Application of ERTS Images and Image Processing to Regional Geologic Problems and Geologic Mapping in Northern Arizona," NASA Technical Report 32-1597, JPL, California Institute of Technology, Pasadena, California, 1975.

Gramenopoulos, N., "Terrain Type Recognition Using ERTS-1 MSS Images," Symposium on Significant Results Obtained from the Earth Resources Technology Satellite, NASA SP-327, March, 1973, 1229-1241.

Haralick, R.M., Shanmugan, K. and I. Dinstein, "Textural Features for Image Classification," IEEE Trans. Systems, Man, and Cybernetics, SMC-3, 1973, 610-621.

Haralick, R.M., "A Resolution Preserving Textural Transform for Images," IEEE Proceedings of the Conference on Computer Graphics, Pattern Recognition, and Data Structure, 1975, 51-61.

Hornung, R.J. and J.A. Smith, "Application of Fourier Analysis to Multi-spectral/spatial Recognition," Management and Utilization of Remote Sensing Data, ASP, Symposium, Sioux Falls, South Dakota, october, 1973.

Hsu, S., "Texture-tone Analysis for Automated Land-use Mapping," Photogrammetric Engineering and Remote Sensing, Vol. 44, No. 11, Nov., 1978, 1393-1404.

Hsu, S., "The Mahalanobis Classier with the Generalized Inverse Approach for Automated Analysis of Imagery Texture Data," Computer Graphic and Image Processing, 9 (1979) 117-134.

Hsu, S. and R. Burright, "Texture Perception and the RADC/Hsu Texture Feature Extractor," Photogrammetric Engineering and Remote Sensing,Vol. 46, No. 8, (1980), 1051-1058.

Hsu, S., On Artificial Intelligence Approaches to Image Exploitation: Some Observations from AI Literature and Experimental Results with Target Cueing and Feature Extraction Tasks, Technical Report for "Feature Recognition and Exploitation Development," F30602-83-R-0041, Rome Air Development, 1983, and SR & E, 305 Main Street, Johnsonc City, New York.

Hsu, S., On the Stable Structure, Textural Regions of Scene and Artificial Intelligence Approaches to Feature Extraction, Target Cueing and Scene Context Analysis with With Data, In-house Technical Report, SR & E, 305 Main Street, Johnson City, New York, 1983. A revised version will be published in Technical Papers, American Society of Photogrammetry, March, 1984.

Hunt, G. and J. Salisbury, "Visible and Near-Infrared Spectra of Minerals and Rocks," Multiple articles in Modern Geology, 1970 through 1971.

Hunt, G., Salisbury, J. and J. Lenhoff, "Visible and Near Infrared Spectra of Menerals and Rocks-IX: Basic and Ultrabasic Igneous Rock,"in Modern Geology, 5:89-95.

Kaizer, H., A Quantification of Texture on Aerial Photographs, Boston University Research Laboratories, Technical Report Note 121, 1955, AD 69484.

Kiracofe, B.E., The Effect of Vegetation on Lithological Discrimination Using Textural Algorithms with LANDSAT Digital Data in the Adirondack Mountains, New York, M.A. Theis, Department of Geography, State University of New York at Binghamton, Binghamton, N.Y., 1983.

Kirvida, L. and G. Johnson,"Automatic Interpretation of Earth Resources Technology Satellite Data for Forest Management," Symposium on Siginificant Results Obtained from the Earth Resources Technology Satellite, NASA SP-327, March, 1973, 1076-1082.

Jules, B.,"Visual Pattern Discrimination," IEEE Trans. Information Theory, IT-8, 1962, 84-92.

Jules, B., "Experiments in the Visual Perception of Texture," Scientific American, 232(4), 1974, 34-43.

Lendaris, G.G. and G.L. Stanley, "Diffraction-pattern Sampling for Automatic Pattern Recognition, Proceedings, IEEE, 58(1970), 198-216.

Lev, A., Zucker, W. and A. Rosenfeld, "Iterative Enhancement of Noisy Images," IEEE Trans. Systems, Man and Cybernetics, SMC-7, 1977, 435-442.

Lipkin, B.S. and A. Rosenfeld,(eds), Picture Processing and Psychopictorics, Academic Press, New York, 1970.

Matheron, G., Elements Pour Une Theorie des Milieux Poreux, Masson, Paris, 1967.

Lyon, R.J.P., "Mineral Exploration Applications of Digitally Processed LANDSAT Imagery," Proceedings, First Annual Pecora Symposium, October, 1975, P.W. Woll and W.A. Fischer (eds), 1977, 271-292.

McCord, T.B., Color Difference on the Lunar Surface, Ph.D. Dissertation, California Institute of Technology, 1968,1-30.

McCord, T.B. and J.A. Westphal, "Two Dimensional Silicon Vidicon Astronomical Photometer," Applied Optics. 11(3), 1972,522-526.

Michell, O.R., Myer, C.R. and W. Boyne," A Max-min Measure for Image Texture Analysis," IEEE Trans. Computers, C-26,1977, 408-414.

Parker, R., Application of Texture-tone Analysis of LANDSAT Data to Geologic Exploration, Senior Thesis at Allegheny College, Pennsylvia, 1980.

Pavlin, G., Computer Programs: HSUDRIVE, TEX13, TEX2, Implementing the Hsu Texture Measures, Pennsylvania State University, 1979.

Pavlin, G. and C.A. Langston, "An Integrated Study of Reservoir-Induced Seismicity and LANDSAT Imagery at Lake Kariba, Africa," Phogrammetric Engineering and Remote Sensing, XLIX(4), April, 1983, 513-526.

Pickett, R.M., "The Perception of Random Visual Texture, " Models for the Perception of Speech and Visual Form (W. Wathen-Dunn, ed.) MIT Press, 1967, 224-232.

Pilot, A., "Computer Generation of Textures," Behavior Research Methods and Instrumentation 8, 1976, 367-368.

Podwysocki, M., The Relationships of Fracture Traces to Geologic Parameters in Flat-lying Sedimentary Rocks: A Statistical Analysis, Ph.D. Thesis, The Pennsylvania State University, 1974.

Purks, S.R. and W. Richards, "Visual Texture Discrimination using Random-dot Patterns," J. Opt. Soc. Am., 67,1977,765-771.

Ravenhurst C.D., Utility of Digitally Merged SEASAT-A SAR, LANDSAT MSS and Magnetic Field Data Sets for Mapping Lithology and Structure in a Vegetaed Terrain, M.S. Thesis, The Pennsylvania State University, 1980.

Richars, W., Experiments in Texture Perception, Annual Report (july, 1977), Contract No. F44620-74-0076, Air Force Office of Scientific Research, Bolling Air Force Base, ARPA Order No. 2765.

Rosenfeld, A., Visual Texture Analysis: An Overview, Technical Report Series, TR-406, University of Maryland, Collelge Park, Maryland, 1975.

Rowan, L.C., Goetz, A.H. and R. Ashley," Discrimination of Hyderothermally Altered and Unaltered Rocks in Visible and Near Infrared Multispectral Images," Geophysics, 42(3), April, 1977, 522-535.

Rowan, L.C., Wetlaufer, P.H., Goetz, A.H., Billingsley, F.C. and J.H. Stewart, "Discrimination of Rock Types and Detection of Hydrothermally Altered Areas in South-central Nevada by the Use of Computer Enhanced ERTS Images," U.S. Geological Survey Professional Paper, 883, U.S. Government Printing Office, Washington, D.C., 1976.

Schachter, B.J. , Lev. A., Zucher, W. and A. Rosenfeld,"An Application of Relaxation Methods to Edge Reinforcement," IEEE Trans. Systems, Man and Cybernetics, SMC-7, 1977, 813-816.

Serra, J. and G. Verchery, "Mathematical Morphology Applied to Fiber Composite Material," Film Science and Technology 6, 1973,141-158.

Weszka, J. and A. Rosenfeld, "A Comparative Study of Texture Measures for Terrain Classification," IEEE Proceedings of the Conference on Computer Graphics, Pattern Recognition and Data Structure, May, 1975,62-64.

OPEN FILE REPORT
81-737

Appendix 1

DISCUSSION re The Quaternary Geologic Map

This map is one of three in the U.S. Geological Survey open-files that emphasize the nature and distribution of upper Quaternary deposits in the Antelope Valley and the adjacent canyons of the Transverse Ranges and Tehachapi Mountains in south-central California (see index map). The area covered by the set of three maps encompasses about 4200 square kilometers of northern Los Angeles County and parts of San Bernardino and Kern Counties, excluding Angeles National Forest and parts of Edwards Air Force Base. Topography in the area ranges from rugged semiarid mountains and steep canyons to broad valleys and arid desert flatlands; elevations range from about 300 meters in valley lowlands to more than 1,800 meters on mountain peaks. About 150,000 people live in the area, with most of the population in the cities and towns of Lancaster, Palmdale, Rosamond, Quartz Hill, Littlerock, Saugus, and Newhall.

The map serves two purposes. Valley and canyon deposits of Quaternary age are those that most affect and are most affected by land-use decisions, and so this map should be useful to planners and engineers as an aid in assessing areas subject to flash floods, foundation and drainage problems, severe ground motion during earthquakes, and other geologic hazards. The distribution, age, and pattern of faulting and folding of the deposits of this map also provide earth scientists with an overview of the nature of sediment deposition and deformation in one of the most tectonically active regions of the world.

This map is designed as a regional appraisal of the distribution and properties of late Quaternary materials. It is accurate for its scale and purpose as an aid to earthquake hazard zonation, land-use planning, and regional tectonic analysis. However, it should be considered only as background information and not as a substitute for large-scale, site-specific studies where land-use and engineering decisions require more detailed geotechnical information.

Upper Quaternary alluvial, colluvial, lacustrine, and eolian deposits are differentiated on the map. These materials have accumulated in the valleys and canyons of the area in response to uplift and erosion of the Transverse Ranges and Tehachapi Mountains and to subsidence of the Antelope Valley Basin during the last half-million years or so. All the upper Quaternary map units are unconsolidated, they have similar, primarily granitic, clast lithologies, and they retain some or all of their original depositional surfaces. These characteristics distinguish the deposits from older Quaternary and pre-Quaternary formations of diverse lithology which are weakly to firmly consolidated and deformed and which preserve none of their original depositional surfaces.

Alluvial deposits of seven major episodes of deposition are the most widely exposed upper Quaternary materials in the area. Correlative colluvium with generally similar textural characteristics and alluvium whose texture has been modified by the addition of windblown sand are shown on the map with distinguishing patterns. Materials deposited during the high stands of shallow lakes, alluvium that has been modified by the addition of large amounts of calcium carbonate around the lake shorelines, and dunes of uniform sand that migrate during dry lake periods occupy the valley lowlands.

We determined the relative ages of the upper Quaternary deposits and the distribution of textural facies in deposits by compilation of U.S. Soil Conservation Service soils maps, by interpretation of aerial photographs, and by study in the field. Preliminary maps were first produced by compiling soils maps of Woodruff and others (1970). Using their descriptions of the major soil series in the region, we were able to identify various ages of the deposits and to obtain approximate grain size distributions in soil parent materials. We could do this because for deposits that still retain some of their original surfaces, the degrees of profile development and textures of the soils directly reflect the relative ages and textures of the deposits upon which the soils formed. The compilation of soils mapping then served as a guide to field inspection of soil samples from channel edge exposures, road cuts, and thousands of shallow auger holes throughout the study area. From this information we determined a sequence of soils and deposits of seven distinct ages. Other criteria such as superposition of deposits, topographic position, and degree of fan surface dissection were also useful for relative dating of deposits, particularly in areas of high relief, structural complexity, and windblown sand veneers.

The grain size distributions within the geologic units differ significantly in some localities from the grain size interpreted from soils descriptions, and we therefore relied on field reconnaissance and the examination of several hundred collected and sieved samples to establish the locations of the facies. Wide variations in grain size over small distances in some of the materials make accurate delineation of facies impossible at map scale, and contacts between facies within units should be considered as only approximately located.

Radiometric ages of the upper Quaternary units are unknown because datable material is very rare in deposits of the area, but we can estimate their ages from stratigraphic position and comparison with dated deposits elsewhere. The Pleistocene Harold Formation, containing land mammal fossils of Rancholabrean age, directly underlies the oldest Q1 deposits in the southeastern part of the area (Noble, 1953; A. G. Barrows, oral communication, 1980). Estimated age of the oldest Rancholabrean fossils is 450,000 years (Repenning, 1980), and the late Quaternary deposits on this map is thus probably no older than about 400,000 years. The ages of upper Quaternary units in the alluvial sequence are estimated on the assumption that the deposits result from climatically controlled episodes of alluviation that are essentially synchronous over broad regions (Ponti, 1980; Ponti and others, 1980). The units are quite extensive and can be recognized along both the Transverse Ranges and Tehachapi mountain fronts in diverse tectonic settings and across the various microclimates of the Antelope Valley and adjacent highlands. They appear to have their origins as pulses of sediment produced during fluctuations of climate from glacial to interglacial times and can be tentatively correlated with climatically controlled deposits in other regions. Good correspondence occurs between the Antelope Valley units and the Riverbank and Modesto formations in the San Joaquin Valley. Q1, Q2, and Q3 deposits appear equivalent to the upper, middle and lower members of the Riverbank Formation, which have estimated ages from 450,000 to 130,000 years (Marchand and Allwardt, 1980). Units Q4, Q5, and Q6 appear equivalent to the Modesto Formation, which has an age estimated to span the period from 90,000 to 9,000 years ago (Marchand and Allwardt, 1980). Lacustrine deposits (Qpl) and calcium carbonate affected alluvium (Quca) result from deposition in and groundwater influences of pluvial lakes which filled the Antelope Valley basin during the most recent (post-Q3) glacial periods. Units Q7, present stream beds (Qs), and sand dunes (Qds) are in part historic and change each season with winter rainfall, summer flash floods, and springtime winds.

Contacts between units beneath upper Quaternary materials are compiled and simplified from large- and intermediate-scale mapping by the U.S. Soil Conservation Service (Woodruff and others, 1970), and from Barrows (1977 and 1980), Barrows and others (1976), Beeby (1977), Dibblee (1960, 1961, 1963, 1967), Jahns and Muehlberger (1954), Kahle (1977), and Kahle and others (1975).

Geologic structures in the Antelope Valley are from unpublished mapping by D. B. Burke and C.W. Hedel, those in the rift zone of the San Andreas fault are from recent studies by the California Division of Mines and Geology (Barrows, 1977 and 1980; Barrows and others, 1976; Beeby (1977); Kahle, 1977; Kahle and others, 1975), those in the Garlock fault zone are from Clark (1973), and those in the San Gabriel Mountains are from Jahns and Muehlberger (1954).